


Dynamics of quantum Fisher information from a time-local non-Markovian master equation with decoherence rates and operators depending on the estimated parameter

Mihaela Vatasescu *Institute of Space Sciences, INFLPR, MG-23, 77125 Bucharest-Magurele, Romania*

(Received 21 February 2022; accepted 27 September 2022; published 10 October 2022)

We analyze the dynamics of the quantum Fisher information (QFI) in the case of a two-dimensional open quantum system obeying a time-local non-Markovian master equation in the canonical form, characterized by canonical decoherence rates and operators that depend on the parameter to be estimated. This last condition brings a framework in which the information about the parameter is structurally encoded not only in the open system, but also in the system-environment interaction or/and correlations, and in some environment properties. We derive analytical formulas for the decompositions of the QFI flow and of the purity dynamics in terms associated to the canonical decoherence rates. In contrast to the results presented in X.-M. Lu *et al.* [*Phys. Rev. A* **82**, 042103 (2010)], we show that, in this extended framework, the QFI flow contains not only the subflows corresponding to the decoherence rates, but also supplementary terms which originate in the state dependence on the estimated parameter; moreover, the signs of the QFI subflows associated to the decoherence rates are not correlated to the signs of the rates. We show that a pertinent connection between the QFI flow and non-Markovianity can be realized using the canonical measures defined from the negative canonical decoherence rates. We employ this theoretical framework to explore the QFI flow and its subflows in two cases of quantum evolutions directed by master equations with decoherence rates or/and operators depending on the estimated parameter: (i) the Markovian nonunitary time evolution of a qubit under the generalized amplitude damping channel; (ii) the non-Markovian time evolution of a two-dimensional electronic subsystem entangled with its vibrational environment in a molecule.

DOI: [10.1103/PhysRevA.106.042204](https://doi.org/10.1103/PhysRevA.106.042204)

I. INTRODUCTION

Quantum Fisher information (QFI) is a central concept in quantum estimation theory [1–6], geometry of quantum states [3,7–9], and quantum metrology [10–13]. QFI connects the achievable precision in the estimation of a parameter encoded in a quantum state to the statistical distinguishability of neighboring quantum states [1,3]. In the quantum Cramér-Rao theorem [14], the lower bound to the estimation precision is provided by the inverse of the QFI. Therefore, quantum evolutions able to increase the QFI are of major interest in quantum metrology with open quantum systems [13].

The estimation of a parameter related to the open system depends on the environmental noise captured by the open system dynamics. The environment properties become essential when the open system is used as a quantum probe (i.e., the estimated parameter is informative about the environment), and when the open system dynamics is non-Markovian. The role of quantum non-Markovianity [15–18] in quantum metrology is an open question, being in general researched using specific noise models [11]. It was argued that, for certain systems and specific settings, non-Markovianity is not necessarily a resource [13,19]. On the other hand, non-Markovian noise was proved to be helpful in quantum-enhanced measurement schemes which use entangled sensors that are fragile due to decoherence [20–22]. Recently, the framework of metrology

of quantum combs was proposed as a general information-theoretic structure for non-Markovian metrology [23].

In order to understand the role of the environmental memory effects on the estimation precision, the dynamics of two-state systems in dissipative environments was investigated by analyzing the time behavior of the QFI in Markovian and non-Markovian regimes [24–30]. The results disclosed various schemes in which non-Markovianity can boost the estimation performance. In contrast to the monotonic behavior of the QFI in the presence of Markovian evolution, the non-Markovian environments produce QFI revivals and retardation of the QFI loss [26,29], or enhancement and preservation of the QFI [28]. QFI oscillations in non-Markovian environments are interpreted as related to the reversed flow of information towards the open system, associated with memory effects.

The connection between the time behavior of the QFI and the non-Markovian character of dynamics has an intrinsic information-theoretic interest, as reflecting the change of information between the open system and the environment. Among the various approaches to the quantum non-Markovianity, one can find the proposals to characterize non-Markovianity using the QFI flow [31], or with the help of a quantum-Fisher-information matrix [32]. In various systems, a positive QFI flow (“incoming flow”) is observed as witnessing non-Markovianity [33–35].

In Ref. [31], the authors showed that “for a class of the non-Markovian master equations in time-local forms,” the QFI flow can be decomposed into additive subflows corresponding

*mihaela_vatasescu@yahoo.com

to different dissipative channels. Consider θ as the parameter to be estimated from a density operator $\rho(\theta; t)$ describing an open quantum system, whose dynamics obeys a time-local master equation with decay rates $\gamma_i(t)$. Taking $F_\theta(t)$ as the QFI associated to θ , Ref. [31] established an expression of the QFI flow as a sum of subflows corresponding to the various decay rates γ_i : $\partial F_\theta/\partial t = \sum_i \gamma_i \mathcal{J}_i$, with $\mathcal{J}_i \leq 0$. Then, the sign of the subflow $\gamma_i \mathcal{J}_i$ is determined by the sign of the decay rate γ_i , such that to a negative γ_i is associated a positive subflow $\gamma_i \mathcal{J}_i$. As a negative decay rate is a defining trait of non-Markovianity, this relation between the QFI subflows and the decay rates installs the positive QFI subflows as significant markers of the non-Markovian behavior. However, this decomposition of the QFI flow into subflows with signs correlated to the signs of the decay rates, it is obtained under certain conditions on the time-local master equation. It can be shown [36] that the decomposition into subflows obtained in Ref. [31] is valid under two conditions not mentioned in the paper: (i) $\frac{d}{dt}(\frac{\partial \rho}{\partial \theta}) = \frac{\partial}{\partial \theta}(\frac{d\rho}{dt})$; (ii) $\frac{\partial H}{\partial \theta} = 0$, $\frac{\partial \gamma_i}{\partial \theta} = 0$, $\frac{\partial A_i}{\partial \theta} = 0$. The first condition may be easily fulfilled if the second partial derivatives are continuous. The second condition refers to the Hamiltonian $H(t)$, the decay rates $\gamma_i(t)$, and the Lindblad operators $A_i(t)$ which characterize the time-local master equation, the result of Ref. [31] being obtained supposing that these quantities do not depend on the parameter θ about which the QFI is defined.

The aim of this work is to explore the extended framework in which γ_i , H , and A_i do depend on θ . In this case, the dynamical map which defines the time evolution of the open system depends on the parameter θ , and therefore the QFI $F_\theta(t)$ can increase in Markovian dynamics. The dependence of the dynamics on the parameter θ [through $H(\theta, t)$, $\gamma_i(\theta, t)$, and $A_i(\theta, t)$] signifies that the coupling between the open system and its environment, and some environment properties, depend on the parameter θ . Therefore, the information about θ is structurally present not only “inside” the open system, but also “outside,” in the environment and its interaction or/and correlations with the open system. As the QFI $F_\theta(t)$ characterizes the information about θ in the open system, the QFI dynamics will reflect a complex sharing of information about θ , between a system and an environment having θ as a “common parameter.”

We shall analyze the QFI flow dF_θ/dt in the case of a two-dimensional open quantum system whose density operator $\rho(\theta; t)$ obeys a time-local non-Markovian master equation in the canonical form [37], with the decoherence rates $\gamma_i(\theta, t)$, the Hamiltonian $H(\theta, t)$, and the decoherence operators $A_i(\theta, t)$, all depending on the estimated parameter θ . We consider a general case in which the operators $A_i(\theta, t)$ may be non-Hermitian, and the generator of the master equation can be nonunitary. The non-Markovianity of the open system dynamics will be characterized using the canonical non-Markovianity quantifiers based on the occurrence of negative decoherence rates in the canonical master equation [37]. We shall consider the QFI dynamics from the point of view of its decomposition into subflows corresponding to the decoherence rates, and we shall analyze its connections to the time evolution of the system’s purity $\mathcal{P} = \text{Tr}(\rho^2)$ or its correlated quantity, the linear entropy $L = 1 - \text{Tr}(\rho^2)$, which may be employed as a measure of the entanglement between the open

system and its environment. The purity of an open system can increase in nonunitary dynamics [38,39], as well as in a non-Markovian evolution. The time derivative of purity will also be investigated as decomposition into terms associated with the decoherence rates.

This theoretical treatment will be applied in the exploration of the QFI dynamics in two cases of quantum evolutions directed by master equations with decoherence rates or/and operators depending on the estimated parameter: (i) the Markovian nonunitary evolution of a qubit under the generalized amplitude damping (GAD) channel [40,41]; (ii) the non-Markovian evolution of a two-dimensional electronic subsystem in the vibrational environment of a molecule [42]. In this last case, we consider an electronic open system entangled with its vibrational environment. We shall analyze the dynamics of the QFI related to the population of an electronic state, which is a parameter encoded in the electronic subsystem, the vibrational environment, and their correlations. The QFI dynamics is explored in relation to the time evolutions of the electronic coherence, the electronic-vibrational entanglement, and the canonical non-Markovianity measure.

The paper has the following structure. In Sec. II are derived the general formulas describing the time derivative of the purity $d\mathcal{P}/dt$, and the QFI flow dF_θ/dt , in terms of the decoherence rates. In Sec. III we analyze the dynamics of the QFI associated to the estimation of the bath temperature, for a qubit evolution under the GAD channel. In Sec. IV is developed the analysis of the QFI related to the electronic population, in the non-Markovian evolution of a two-dimensional electronic subsystem in the vibrational environment of a molecule. Section V assembles our final remarks.

II. QUANTUM FISHER INFORMATION AND PURITY IN THE EVOLUTION OF AN OPEN QUANTUM SYSTEM OBEYING A TIME-LOCAL NON-MARKOVIAN MASTER EQUATION IN THE CANONICAL FORM

Suppose an open quantum system with the density operator $\rho(\theta; t)$, where θ is a parameter to be estimated, whose dynamics obeys a time-local non-Markovian master equation in the canonical form [37]

$$\frac{d\rho}{dt} = -\frac{i}{\hbar}[H(\theta; t), \rho] + \sum_{i=1}^{N-1} \gamma_i(\theta; t) \left[A_i(\theta; t) \rho A_i^\dagger(\theta; t) - \frac{1}{2} \{A_i^\dagger(\theta; t) A_i(\theta, t), \rho\} \right], \quad (1)$$

where the Hamiltonian $H(\theta; t)$, the decoherence operators $A_i(\theta; t)$, and the decoherence rates $\gamma_i(\theta; t)$ are in general time dependent, and may depend on the estimated parameter θ . The decoherence operators A_i ($i = 1, \dots, N-1$, with $N := d^2$, d the dimension of the open system) form an orthonormal basis set of traceless operators [37]:

$$\text{Tr}[A_i] = 0, \quad \text{Tr}[A_j^\dagger A_k] = \delta_{jk}. \quad (2)$$

The canonical decoherence rates $\gamma_i(\theta; t)$ are uniquely determined, and they can be used to characterize the non-Markovianity of the time evolution [37]. The definition of non-Markovianity used here is the one given in Ref. [37], namely, the time evolution is non-Markovian if at least one

of the canonical decoherence rates is strictly negative. We shall employ the measures of non-Markovianity defined in Ref. [37] as functions of the negative canonical decoherence rates $\gamma_i(\theta; t)$. The canonical measure of non-Markovianity at time t is defined as the sum of the measures coming from all individual channels characterized by negative decay rates: $f(\theta; t) = \sum_i f_i(\theta; t)$, with $f_i(\theta; t) := \max[0, -\gamma_i(\theta; t)]$. The total amount of non-Markovianity over a time interval $[t, t']$ is defined as $\int_t^{t'} f(s) ds$. Let us observe that, from its definition, the canonical measure of non-Markovianity $f(\theta, t)$ is a function of the parameter θ .

A. Quantum Fisher information for a two-dimensional open quantum system

Among various QFI versions, as different extensions from the classical Fisher information, the symmetric logarithmic derivative QFI distinguishes itself as being obtained by the maximization of the classical Fisher information over all quantum measurements independent of θ , and leading to the quantum Cramér-Rao inequality [1–4, 43]. The symmetric logarithmic derivative QFI defines a distinguishability metric in the space of quantum states, being proportional to the Bures metric, which gives the statistical Bures distance between two quantum states, obtained by an infinitesimal change in the parameter θ [3, 4].

The symmetric logarithmic derivative QFI corresponding to a parameter θ to be estimated is [1, 2]

$$F_\theta = \text{Tr}[\rho(\theta)L_\theta^2] = \text{Tr}\left[\frac{\partial\rho(\theta)}{\partial\theta}L_\theta\right], \quad (3)$$

where L_θ is the symmetric logarithmic derivative (SLD) [1], also known as quantum score, defined as the Hermitian operator satisfying the equation

$$\frac{\partial\rho(\theta)}{\partial\theta} = \frac{\rho(\theta)L_\theta + L_\theta\rho(\theta)}{2}. \quad (4)$$

The definition (4) implies that the mean value of the operator L_θ vanishes, $\text{Tr}[\rho(\theta)L_\theta] = 0$.

The quantum Cramér-Rao inequality gives the lower bound to the estimation precision of θ as [1–3]

$$\text{Var}(\theta) \geq \frac{1}{MF_\theta}, \quad (5)$$

where Var denotes the variance, and M is the number of measurements performed. Equation (5) defines the quantum Cramér-Rao bound (QCRB) for the variance of an unbiased estimator.

The QFI has important properties [9, 10], one of them being that it does not increase under completely positive and trace-preserving (CPTP) maps that do not depend on the parameter θ . Our working hypothesis of a dynamics directed by Eq. (1), in which all the significant quantities depend on θ , implies that the map depends on the parameter θ . We shall follow F_θ as a dynamical quantity determined by the evolution (1) of the open system.

In the Bloch representation, the density operator $\rho(\theta; t)$ of a two-dimensional open system is given by

$$\rho(\theta; t) = \frac{1}{2}(\hat{I} + \vec{\omega}(\theta; t) \cdot \vec{\sigma}), \quad (6)$$

with \hat{I} the identity operator, $\vec{\omega} = (\omega_1, \omega_2, \omega_3)$ the real three-dimensional Bloch vector, and $\vec{\sigma} = (\sigma_1, \sigma_2, \sigma_3)$ the vector assembling the three Pauli operators σ_i . The Euclidean norm of the Bloch vector $|\vec{\omega}|$ determines the purity of the open system,

$$\mathcal{P} = \text{Tr}(\rho^2) = (1 + |\vec{\omega}|^2)/2, \quad (7)$$

as well as the linear entropy $L = 1 - \text{Tr}(\rho^2)$,

$$L = (1 - |\vec{\omega}|^2)/2, \quad (8)$$

which, when it is the case, may be employed as measure of the entanglement between the open system and its environment.

For a two-dimensional quantum system with the quantum state (6), the QFI for the parameter θ is [24, 44]

$$F_\theta = |\partial_\theta \vec{\omega}|^2 + \frac{(\vec{\omega} \cdot \partial_\theta \vec{\omega})^2}{1 - |\vec{\omega}|^2}, \quad |\vec{\omega}| < 1, \quad (9)$$

with $\partial_\theta \vec{\omega} = \frac{\partial \vec{\omega}}{\partial \theta}$. If $|\vec{\omega}| = 1$ (pure state), $F_\theta = |\partial_\theta \vec{\omega}|^2$.

Reference [44] shows that F_θ given by Eq. (9) is a function which increases with $|\vec{\omega}|$, therefore, the increase of the purity \mathcal{P} of a qubit state is favorable to the QFI increase. In the following we shall explore the relation between the time derivative of the QFI F_θ and the time derivative of the purity \mathcal{P} , on general formulas, as well as in specific cases of dynamics.

The quantum score L_θ in Bloch representation has the form

$$L_\theta = a\hat{I} + \vec{b} \cdot \vec{\sigma}, \quad (10)$$

where a and the three-component vector $\vec{b} = (b_1, b_2, b_3)$ are real-valued functions of the parameter θ and of time t , having the expressions [44]

$$a = -\frac{\vec{\omega} \cdot \partial_\theta \vec{\omega}}{1 - |\vec{\omega}|^2}, \quad \vec{b} = -a\vec{\omega} + \partial_\theta \vec{\omega}. \quad (11)$$

Let us observe that $F_\theta = |\vec{b}|^2 - a^2$, and $a = -\vec{\omega} \cdot \vec{b}$.

B. Decomposing the QFI flow and the purity dynamics in terms corresponding to the decoherence rates

The QFI definition (3) and the expression of the quantum score (10) give $F_\theta = \vec{b} \cdot \frac{\partial \vec{\omega}}{\partial \theta}$ and, therefore, the time derivative of F_θ can be written as

$$\frac{dF_\theta}{dt} = \vec{b} \cdot \frac{d}{dt} \left(\frac{\partial \vec{\omega}}{\partial \theta} \right) + \frac{\partial \vec{\omega}}{\partial \theta} \cdot \frac{d\vec{b}}{dt}. \quad (12)$$

Using Eqs. (11) and (12) we get

$$\frac{dF_\theta}{dt} = 2a^2 \frac{d\mathcal{P}}{dt} - 2a \frac{\partial \vec{\omega}}{\partial \theta} \cdot \frac{d\vec{\omega}}{dt} + 2\vec{b} \cdot \frac{d}{dt} \left(\frac{\partial \vec{\omega}}{\partial \theta} \right), \quad (13)$$

where the time derivative of the open system purity is

$$\frac{d\mathcal{P}}{dt} = 2 \text{Tr} \left(\rho \frac{d\rho}{dt} \right) = \vec{\omega} \cdot \frac{d\vec{\omega}}{dt}. \quad (14)$$

Equations (13) and (14) can be developed by expressing $\frac{d\omega_j}{dt}$ as a function of the decoherence rates γ_i . Equation (6) implies

$$\frac{d\omega_j}{dt} = \text{Tr} \left(\frac{d\rho}{dt} \sigma_j \right), \quad (15)$$

and using Eq. (1), one obtains

$$\begin{aligned} \frac{d\omega_j}{dt} = & \frac{1}{\hbar} \sum_{i=1}^3 \varepsilon_{ijk} \omega_i \text{Tr}(H\sigma_k) - \frac{1}{2} \omega_j \sum_{i=1}^3 \gamma_i \\ & + \frac{1}{2} \sum_{i=1}^3 \gamma_i \text{Tr}([A_i, A_i^+] + A_i \vec{\omega} \cdot \vec{\sigma} A_i^+) \sigma_j, \end{aligned} \quad (16)$$

where ε_{ijk} is the Levi-Civita symbol.

1. Purity dynamics in terms of the decoherence rates

We begin by examining the time derivative of the purity. Equations (14) and (16) give $\frac{d\mathcal{P}}{dt} = \sum_j \omega_j \frac{d\omega_j}{dt}$ as a function of the decoherence rates γ_i :

$$\begin{aligned} \frac{d\mathcal{P}}{dt} = & -\frac{|\vec{\omega}|^2}{2} \left(\sum_i \gamma_i \right) \\ & + \frac{1}{2} \sum_i \gamma_i \text{Tr}([A_i, A_i^+] + A_i \vec{\omega} \cdot \vec{\sigma} A_i^+) \vec{\omega} \cdot \vec{\sigma}. \end{aligned} \quad (17)$$

The decoherence operators A_i can be written using the Pauli operators as $A_i = c_i \hat{I} + \vec{d}^{(i)} \cdot \vec{\sigma}$, with c_i complex numbers, and $\vec{d}^{(i)}$ three-component complex vectors. Taking into account the conditions (2), one obtains $c_i = 0$ and

$$A_i = \sum_j d_j^{(i)} \sigma_j, \quad (18)$$

with the complex components $d_j^{(i)}$ ($j = 1, 2, 3$) obeying

$$\sum_j |d_j^{(i)}|^2 = \frac{1}{2}. \quad (19)$$

Equation (17) can be transformed using Eqs. (18) and (19) to write $\text{Tr}(A_i \vec{\omega} \cdot \vec{\sigma} A_i^+ \vec{\omega} \cdot \vec{\sigma}) = 4(\vec{d}^{(i)} \cdot \vec{\omega})(\vec{d}^{(i)*} \cdot \vec{\omega}) - |\vec{\omega}|^2$. Using the Cauchy-Schwarz inequality $|\sum_j d_j^{(i)} \omega_j|^2 \leq \sum_j |d_j^{(i)}|^2 \sum_j |\omega_j|^2$ and Eq. (19), one obtains

$$q_i = |\vec{\omega}|^2 - 2(\vec{d}^{(i)} \cdot \vec{\omega})(\vec{d}^{(i)*} \cdot \vec{\omega}) \geq 0. \quad (20)$$

Finally, $d\mathcal{P}/dt$ can be written as a sum of subflows corresponding to the decoherence rates γ_i :

$$\frac{d\mathcal{P}}{dt} = \sum_i \gamma_i [-q_i + \text{Tr}([A_i, A_i^+] \rho)], \quad (21)$$

with $q_i \geq 0$ given by Eq. (20). Equation (21) describes a general case, with decoherence rates $\gamma_i(t)$ that can be negative (non-Markovian dynamics), and non-Hermitian time-dependent decoherence operators A_i .¹

Reference [38] shows that in quantum Markovian dynamics, for finite-dimensional Hilbert spaces, the purity is monotonically decreasing if and only if the Lindblad generator is unital. The condition of unitality on the generator of the master equation (1) is

$$\sum_i \gamma_i [A_i, A_i^+] = 0. \quad (22)$$

If the unitality condition (22) is fulfilled, we get $d\mathcal{P}/dt = -\sum_i \gamma_i q_i$, monotonically decreasing if all $\gamma_i > 0$. Obviously, the purity can increase in non-Markovian dynamics (where at least one decoherence rate γ_i is negative), and in nonunital dynamics.

Equation (21) can also be written

$$\frac{d\mathcal{P}}{dt} = \sum_i \gamma_i - 2 \sum_i \gamma_i q_i' + \sum_i \gamma_i \text{Tr}([A_i, A_i^+] \rho), \quad (23)$$

with $q_i' = \text{Tr} \rho^2 - |\text{Tr}(\rho A_i)|^2 \geq 0$. Equation (23) is obtained using Eq. (2) and the Cauchy-Schwarz inequality $\text{Tr}(AA^+) \text{Tr}(BB^+) \geq |\text{Tr}(AB^+)|^2$ for the operators $A = \rho$, $B = A_i$. The last expression makes appear the sum of the decoherence rates $\sum_i \gamma_i$, which determines the behavior of the Bloch volume of the states dynamically accessible to the system [37]. A negative sum of the decoherence rates constitutes a quantity with meaning in witnessing quantum non-Markovianity through the increase of the Bloch volume [37,45].

2. QFI dynamics in terms of the decoherence rates and supplementary terms

If the time derivative of the QFI given in Eq. (13) is developed using Eq. (16) to express the term $\frac{\partial \vec{\omega}}{\partial \theta} \cdot \frac{d\vec{\omega}}{dt} = \sum_j \frac{\partial \omega_j}{\partial \theta} \frac{d\omega_j}{dt}$, one obtains

$$\begin{aligned} \frac{dF_\theta}{dt} = & 2a^2 \frac{d\mathcal{P}}{dt} - 2a^2 L \sum_i \gamma_i \\ & - a \sum_i \gamma_i \text{Tr} \left[([A_i, A_i^+] + A_i \vec{\omega} \cdot \vec{\sigma} A_i^+) \frac{\partial \vec{\omega}}{\partial \theta} \cdot \vec{\sigma} \right] \\ & + 2\vec{b} \cdot \frac{d}{dt} \left(\frac{\partial \vec{\omega}}{\partial \theta} \right) - \frac{2a}{\hbar} \sum_{i,j} \varepsilon_{ijk} \omega_i \frac{\partial \omega_j}{\partial \theta} \text{Tr}(H\sigma_k). \end{aligned} \quad (24)$$

Equation (24) indicates that the time increase of the purity contributes to the time increase of F_θ . Replacing $d\mathcal{P}/dt$ with Eq. (17), we get

$$\begin{aligned} \frac{dF_\theta}{dt} = & -a^2 \sum_i \gamma_i \\ & - a \sum_i \gamma_i \text{Tr}([A_i, A_i^+] + A_i \vec{\omega} \cdot \vec{\sigma} A_i^+) \vec{b} \cdot \vec{\sigma} \\ & + 2\vec{b} \cdot \frac{d}{dt} \left(\frac{\partial \vec{\omega}}{\partial \theta} \right) - \frac{2a}{\hbar} \sum_{i,j} \varepsilon_{ijk} \omega_i \frac{\partial \omega_j}{\partial \theta} \text{Tr}(H\sigma_k). \end{aligned} \quad (25)$$

Equation (25) shows that dF_θ/dt cannot be decomposed as a sum of subflows corresponding to the decoherence rates γ_i . Indeed, only the first two terms on the right side of Eq. (25), originating in $d\rho/dt$, compose subflows corresponding to γ_i ; but the signs of these subflows cannot be correlated to the signs of their respective decoherence rates. The other two terms are subflows originating in the partial derivative $\partial \rho / \partial \theta$ and its time derivative. The examples following in the next sections will show that all the subflows can become positive or negative during the dynamics. Equation (25) suggests that a non-Markovian dynamics characterized by a

¹The first term is given as expression for the rate of change of the purity in Ref. [64], which considers Hermitian Lindblad operators A_i .

negative sum, $\sum_i \gamma_i < 0$, participates in the increase of the QFI F_θ .

3. Conditions giving the QFI flow as a sum of subflows corresponding to different decoherence channels

It can be shown that Eq. (25) takes the form

$$\frac{dF_\theta}{dt} = - \sum_i \gamma_i \text{Tr}\{\rho[L_\theta, A_i]^+[L_\theta, A_i]\} \quad (26)$$

established in Ref. [31], with $-\text{Tr}\{\rho[L_\theta, A_i]^+[L_\theta, A_i]\} \leq 0$, if the following two conditions are fulfilled [36]:

(i)

$$\frac{d}{dt} \left(\frac{\partial \rho}{\partial \theta} \right) = \frac{\partial}{\partial \theta} \left(\frac{d\rho}{dt} \right). \quad (27)$$

(ii) γ_i, H, A_i do not depend on θ :

$$\frac{\partial H}{\partial \theta} = 0, \quad \frac{\partial \gamma_i}{\partial \theta} = 0, \quad \frac{\partial A_i}{\partial \theta} = 0. \quad (28)$$

As explained in the Introduction, these are the conditions presupposed in the demonstration of Eq. (26), in which the QFI flow dF_θ/dt can be written as a sum of subflows corresponding to the decoherence channels, with the sign of each subflow correlated to the sign of the corresponding $\gamma_i(t)$. With the conditions (i) and (ii), Eq. (25) is simplified giving Eq. (26), with

$$\begin{aligned} \text{Tr}\{\rho[L_\theta, A_i]^+[L_\theta, A_i]\} &= |\vec{b}|^2 \\ &+ a \text{Tr}([A_i, A_i^+]\vec{b} \cdot \vec{\sigma}) - \text{Tr}(A_i \vec{b} \cdot \vec{\sigma} A_i^+ \vec{b} \cdot \vec{\sigma}). \end{aligned} \quad (29)$$

In the following sections we analyze two examples of open system dynamics directed by a time-local master equation of type (1): (I) the Markovian nonunital evolution of a qubit under the GAD channel; (II) the non-Markovian evolution of

the electronic subsystem in the vibrational environment of a molecule.

III. QFI DYNAMICS IN A QUBIT EVOLUTION UNDER THE GENERALIZED AMPLITUDE DAMPING CHANNEL

The generalized amplitude damping (GAD) channel describes the interaction of a qubit (a two-level system with ground state $|g\rangle$ and excited state $|e\rangle$) with a thermal bath modeled as a reservoir of noninteracting bosons [40,46,47], being defined by the quantum operation $\mathcal{E}_{\text{GAD}}(\rho) = \sum_i E_i \rho E_i^\dagger$, with the Kraus operators E_i ($i = 0, \dots, 3$) [41]:

$$\begin{aligned} E_0 &= \sqrt{p} \begin{pmatrix} 1 & 0 \\ 0 & \sqrt{1-\gamma} \end{pmatrix}, \quad E_1 = \sqrt{p} \begin{pmatrix} 0 & \sqrt{\gamma} \\ 0 & 0 \end{pmatrix}, \\ E_2 &= \sqrt{1-p} \begin{pmatrix} \sqrt{1-\gamma} & 0 \\ 0 & 1 \end{pmatrix}, \quad E_3 = \sqrt{1-p} \begin{pmatrix} 0 & 0 \\ \sqrt{\gamma} & 0 \end{pmatrix}. \end{aligned} \quad (30)$$

The two couples of Kraus operators $(E_0, E_1), (E_2, E_3)$ describe the two opposite processes in which the qubit exchanges energy with the thermal bath, both taking place with the same damping rate $\gamma \in [0, 1]$: in the first one, with the occurrence probability p , the qubit decays from the excited to the ground state; in the other, with the probability $1 - p$, the qubit absorbs an excitation from the reservoir, passing from the ground state to the excited state. The probability $p \in [0, 1]$ is a parameter depending on the bath temperature [40,46,47]. The decay rate $\gamma(t)$ depends on the interaction time t with the environment:

$$\gamma(t) = 1 - e^{-\Gamma t}, \quad (31)$$

with Γ a constant characterizing the speed of dissipation [47].

For a qubit initially prepared in a state $\rho(0)$ with the Bloch vector $\vec{r}_0 = (r_x, r_y, r_z)$, GAD performs the transformation $\vec{r}_0 \rightarrow \vec{r}(t) = (r_1, r_2, r_3)$ with [41]

$$\vec{r}(t) = (r_x \sqrt{1-\gamma}, r_y \sqrt{1-\gamma}, \gamma(2p-1) + r_z(1-\gamma)). \quad (32)$$

The qubit state $\rho(t)$ is described by the matrix

$$(\rho(t))_{|g,e\rangle} = \begin{pmatrix} 1 - \gamma(2p-1) - r_z(1-\gamma) & r_x \sqrt{1-\gamma} + i r_y \sqrt{1-\gamma} \\ r_x \sqrt{1-\gamma} - i r_y \sqrt{1-\gamma} & 1 + \gamma(2p-1) + r_z(1-\gamma) \end{pmatrix}. \quad (33)$$

Taking into account Eq. (31), it can be shown that $\rho(t)$ obeys the following master equation:

$$\begin{aligned} \frac{d\rho}{dt} &= \Gamma(1-p) \left(\sigma_- \rho \sigma_+ - \frac{1}{2} \{ \sigma_+ \sigma_-, \rho \} \right) \\ &+ \Gamma p \left(\sigma_+ \rho \sigma_- - \frac{1}{2} \{ \sigma_- \sigma_+, \rho \} \right), \end{aligned} \quad (34)$$

with $\sigma_+ = |e\rangle\langle g|$, $\sigma_- = |g\rangle\langle e|$. The master equation (34) for the GAD dissipative process describes a Markovian dynamics implying two positive and time-independent decoherence rates $\gamma_1, \gamma_2 \geq 0$:

$$\gamma_1 = \Gamma(1-p), \quad \gamma_2 = \Gamma p. \quad (35)$$

The decoherence operators are $A_1 = \sigma_-$ and $A_2 = \sigma_+$, and therefore $\sum_i \gamma_i [A_i, A_i^\dagger] = \Gamma(2p-1)\sigma_3$. Consequently, the GAD channel is nonunital, unless $\Gamma = 0$ or $2p-1 = 0$.²

The decoherence rates $\{\gamma_i\}_{i=1,2}$ depend on the two parameters which characterize the qubit interaction with the bath, the damping constant Γ , and the parameter p related to the bath

²Reference [39] discusses the nonunital non-Markovianity of a quantum process, and illustrates it with a GAD process with a time-dependent $p(t)$. A non-Markovian GAD channel with time dependent $p(t)$ is also studied in Ref. [65].

temperature:

$$\frac{\partial \gamma_i}{\partial \Gamma} \neq 0, \quad \frac{\partial \gamma_i}{\partial p} \neq 0 \quad (i = 1, 2), \quad (36)$$

such that the condition (28) is violated for both parameters Γ and p .

To our knowledge, the interest in the estimation of each of the parameters Γ and p (in the sense of single-parameter estimation) appears in the specific literature in two different contexts. Reference [48] explores the optimality of an estimation scheme for the damping rate γ of a GAD channel in the theoretical framework of the optimal estimation of quantum channels [49,50]. On the other hand, the GAD channel was employed as a phenomenological model in qubit thermometry, to investigate the use of a single qubit (prepared in various initial states) as a thermometer able to distinguish between two temperatures of a bosonic bath [46,47].

Here we shall discuss the dynamics of the QFI $F_p(t)$ for the parameter p related to the bath temperature, as well as the decompositions of dF_p/dt and $d\mathcal{P}/dt$ into subflows corresponding to $\{\gamma_i\}_{i=1,2}$. It is an interesting specificity occurring in the case of the GAD channel that the decoherence rates γ_1, γ_2 [Eq. (35)] are proportional to the probabilities $1 - p$ and p of the opposite processes in which the qubit exchanges energy with the bath, p being also the parameter to be estimated. Therefore, the QFI and the purity subflows are proportional to p and $1 - p$.

Using Eq. (9), $F_p(t)$ can be found as

$$F_p(t) = 4\gamma^2 \frac{1 - (r_1^2 + r_2^2)}{1 - |\vec{r}|^2}, \quad (37)$$

with $\vec{r}(t) = (r_1, r_2, r_3)$ the Bloch vector given in Eq. (32).

Applying Eq. (25) in the GAD case ($\gamma_1 + \gamma_2 = \Gamma$), one obtains the decomposition of the QFI flow into subflows corresponding to the two decoherence rates γ_1, γ_2 :

$$\frac{dF_p}{dt} = \gamma_1 f_1 + \gamma_2 f_2, \quad (38)$$

where f_1, f_2 are the following functions of γ and p :

$$f_1(\gamma, p) = -a^2 + ab_3(2 + r_3) + 4b_3(1 - \gamma), \quad (39)$$

$$f_2(\gamma, p) = -a^2 - ab_3(2 - r_3) + 4b_3(1 - \gamma). \quad (40)$$

a and $\vec{b} = (b_1, b_2, b_3)$ are defined in Eq. (11), and take the following forms for the GAD channel:

$$a = -\frac{2\gamma r_3}{1 - |\vec{r}|^2}, \quad \vec{b} = (-ar_1, -ar_2, -ar_3 + 2\gamma). \quad (41)$$

The qubit purity is $\mathcal{P}(t) = [1 + |\vec{r}(t)|^2]/2$ [Eq. (7)]. With Eq. (23), its time derivative can be decomposed as

$$\frac{d\mathcal{P}}{dt} = \gamma_1 p_1 + \gamma_2 p_2, \quad (42)$$

with $p_1 = -(\frac{|\vec{r}|^2 + r_3^2}{2} + r_3)$ and $p_2 = -(\frac{|\vec{r}|^2 + r_3^2}{2} - r_3)$.

In the following we shall analyze the signs of the QFI and purity subflows. We shall examine the behavior of these quantities in the time evolution of the GAD process considering three initial states $\rho(0)$: the maximally mixed state $\rho(0) = \frac{1}{2}\hat{I}$,

and the pure states $|g\rangle\langle g|$ and $|e\rangle\langle e|$. The results are displayed in Table I.

A. Initial state of the qubit $\rho(0) = \frac{1}{2}\hat{I}$

Let us consider as initial state of the qubit the maximally mixed state

$$\rho(0) = \frac{1}{2}\hat{I} = \frac{1}{2}(|g\rangle\langle g| + |e\rangle\langle e|). \quad (43)$$

The components of the Bloch vector at $t = 0$ are $r_x = r_y = r_z = 0$, and after a time t of interaction with the bath, the Bloch vector (32) becomes $\vec{r}(t) = (0, 0, \gamma(2p - 1))$, with

$$r_3^I = \gamma(2p - 1). \quad (44)$$

The superscript I in Eq. (44) is indicative of the initial state.

The purity is $\mathcal{P}^I(t) = [1 + |r_3^I(t)|^2]/2$, with its time derivative

$$\frac{d\mathcal{P}^I}{dt} = \Gamma e^{-\Gamma t} \gamma (2p - 1)^2 \geq 0. \quad (45)$$

Unsurprisingly, as the initial state is the maximally mixed state, the purity increases in time, $d\mathcal{P}^I/dt \geq 0$. The signs of the purity subflows composing $d\mathcal{P}^I/dt$ [Eq. (42)] are determined by $p_1 = -r_3^I(1 + r_3^I)$ and $p_2 = r_3^I(1 - r_3^I)$, with $\text{sgn}[p_2] = \text{sgn}[r_3^I] = -\text{sgn}[p_1]$. Therefore, the purity subflows $\gamma_1 p_1$ and $\gamma_2 p_2$ have always opposite signs, reflecting their relation with the opposite processes $|g\rangle \rightarrow |e\rangle$ (probability $1 - p$) and $|e\rangle \rightarrow |g\rangle$ (probability p).

The QFI $F_p^I(t)$ [Eq. (37)] and its time derivative dF_p^I/dt are

$$F_p^I(t) = \frac{4\gamma^2}{1 - (r_3^I)^2}, \quad (46)$$

$$\frac{dF_p^I}{dt} = \frac{8\Gamma\gamma(1 - \gamma)}{[1 - (r_3^I)^2]^2} \geq 0. \quad (47)$$

The positive flow $dF_p^I/dt \geq 0$ shows that the accuracy in the estimation of the parameter p increases with time.

The functions f_1, f_2 which determine the signs of the subflows in the QFI flow decomposition (38) are

$$f_1(\gamma, p) = \frac{8\gamma}{(1 - r_3^I)^2} (1 + r_3)(1 - r_3 - \gamma), \quad (48)$$

$$f_2(\gamma, p) = \frac{8\gamma}{(1 - r_3^I)^2} (1 - r_3)(1 + r_3 - \gamma). \quad (49)$$

As $|r_3| < 1$, $\text{sgn}[f_1] = \text{sgn}[1 - r_3 - \gamma]$, and $\text{sgn}[f_2] = \text{sgn}[1 + r_3 - \gamma]$.

The value of p indicates which one of the two opposite processes is dominant (i.e., occurs with bigger probability): it is $|g\rangle \rightarrow |e\rangle$ if $1 - p > p$, or $|e\rangle \rightarrow |g\rangle$ if $p > 1 - p$. In order to enlighten the dominant process, the analysis shown in the Table I is organized by distinguishing the following cases for the parameter $0 \leq p \leq 1$.

(i) If $p < \frac{1}{2}$ (i.e., $1 - p > p$ and $\gamma_1 > \gamma_2$), the process $|g\rangle \rightarrow |e\rangle$ is dominant. The subflows associated with the bigger probability, $1 - p$, are positive: $\gamma_1 p_1 > 0, \gamma_1 f_1 > 0$. The subflow $f_2 > 0$ if $e^{-\Gamma t} > 1 - \frac{1}{2(1-p)}$, and becomes negative,

TABLE I. The signs of the subflows $\gamma_1 f_1$ and $\gamma_2 f_2$ composing the positive QFI flow $\frac{dF_p}{dt} = \gamma_1 f_1 + \gamma_2 f_2 > 0$, and the sign of the time derivative of the purity $\frac{d\mathcal{P}}{dt}$ in the GAD time evolution, for the initial states $\rho(0) = \frac{1}{2}\hat{f}$, $|g\rangle\langle g|$, $|e\rangle\langle e|$. The decoherence rates are $\gamma_1 = \Gamma(1-p)$ and $\gamma_2 = \Gamma p$. We distinguish the cases $2p < 1$ (i.e., $1-p > p$) and $2p > 1$ (i.e., $1-p < p$).

Initial state	p domain	$\text{sgn}[f_1]$	$\text{sgn}[f_2]$	$\text{sgn}[\frac{d\mathcal{P}}{dt}]$
$\frac{1}{2}\hat{f}$	$2p < 1$	$f_1 > 0$	$f_2 > 0$, if $e^{-\Gamma t} > \frac{1-2p}{2(1-p)}$ $f_2 < 0$, if $e^{-\Gamma t} < \frac{1-2p}{2(1-p)}$	$\frac{d\mathcal{P}}{dt} \geq 0$
	$2p > 1$	$f_1 > 0$, if $e^{-\Gamma t} > \frac{2p-1}{2p}$ $f_1 < 0$, if $e^{-\Gamma t} < \frac{2p-1}{2p}$	$f_2 > 0$	$\frac{d\mathcal{P}}{dt} < 0$, if $e^{-\Gamma t} > \frac{2p-1}{2p}$ $\frac{d\mathcal{P}}{dt} > 0$
$ g\rangle\langle g $	$2p < 1$	$f_1 > 0$	$f_2 < 0$	$\frac{d\mathcal{P}}{dt} < 0$, if $e^{-\Gamma t} > \frac{2p-1}{2p}$
	$2p > 1$	$f_1 > 0$, if $e^{-\Gamma t} > \frac{2p-1}{2p+1}$ $f_1 < 0$, if $e^{-\Gamma t} < \frac{2p-1}{2p+1}$	$f_2 > 0$	$\frac{d\mathcal{P}}{dt} > 0$
$ e\rangle\langle e $	$2p < 1$	$f_1 > 0$	$f_2 > 0$, if $e^{-\Gamma t} > \frac{1-2p}{3-2p}$ $f_2 < 0$, if $e^{-\Gamma t} < \frac{1-2p}{3-2p}$	$\frac{d\mathcal{P}}{dt} < 0$, if $e^{-\Gamma t} > \frac{1-2p}{2(1-p)}$
	$2p > 1$	$f_1 < 0$	$f_2 > 0$	$\frac{d\mathcal{P}}{dt} > 0$ $\frac{d\mathcal{P}}{dt} < 0$

$f_2 < 0$, if $e^{-\Gamma t} < 1 - \frac{1}{2(1-p)}$. This indicates that, after a certain time of the interaction with the bath ($t > t^*$), when $e^{-\Gamma t}$ becomes sufficiently small, the subflow associated with the smaller probability p becomes negative, $\gamma_2 f_2 < 0$, showing that the occurrence of the process $|e\rangle \rightarrow |g\rangle$, with probability p , diminishes $F_p(t)$ and the precision in the estimation of p .

(ii) If $p > \frac{1}{2}$ (i.e., $p > 1-p$ and $\gamma_1 < \gamma_2$), the process $|e\rangle \rightarrow |g\rangle$ is the dominant one. It is the inverse of the case (i). The signs of the purity subflows are inverted, with $p_1 < 0$ and $p_2 > 0$. The QFI subflow $\gamma_2 f_2 > 0$, and $\gamma_1 f_1$ becomes negative after a certain time.

(iii) If $p = \frac{1}{2}$, the GAD channel becomes unital, $r_3 = 0$, $p = 1-p$, $\gamma_1 = \gamma_2$, $f_1 = f_2 > 0$. Moreover, $d\mathcal{P}^I/dt = 0$, with $p_1 = p_2 = 0$.

B. Initial state of the qubit $\rho(0) = |g\rangle\langle g|$ or $\rho(0) = |e\rangle\langle e|$

If the qubit is initially prepared in the ground state $\rho(0) = |g\rangle\langle g|$, then $r_x = r_y = 0$ and $r_z = -1$, and the Bloch vector (32) becomes $\vec{r}(t) = (0, 0, 2p\gamma - 1)$, with

$$r_3^g = 2p\gamma - 1. \quad (50)$$

The time derivative of the purity $\mathcal{P}^g(t)$ is

$$\frac{d\mathcal{P}^g}{dt} = 2\Gamma e^{-\Gamma t} p(2p\gamma - 1). \quad (51)$$

As the initial state is the pure state $|g\rangle\langle g|$, the purity begins by decreasing in the time evolution, but it can increase after a certain time if the transition $|e\rangle \rightarrow |g\rangle$ becomes the dominant process ($p > 1-p$): $d\mathcal{P}^g/dt > 0$ if $e^{-\Gamma t} < \frac{2p-1}{2p}$. The purity subflows $\gamma_1 p_1$ and $\gamma_2 p_2$ have always opposite signs, with $p_1 = -r_3^g(1+r_3^g)$ and $p_2 = r_3^g(1-r_3^g)$.

$F_p^g(t)$ and its time derivative dF_p^g/dt are

$$F_p^g(t) = \frac{4\gamma^2}{1 - (r_3^g)^2}, \quad (52)$$

$$\frac{dF_p^g}{dt} = \frac{16p\Gamma\gamma^2(1-\gamma)}{[1 - (r_3^g)^2]^2} \geq 0. \quad (53)$$

f_1 and f_2 have the same expressions as those given in Eqs. (48) and (49), with r_3 taking the value given by Eq. (50). The signs of f_1 and f_2 are shown in Table I. If $p < \frac{1}{2}$, the transition $|g\rangle \rightarrow |e\rangle$ is the dominant process, leading to the decrease of the purity. The purity subflows and the QFI subflows have the same signs: $\gamma_1 p_1 > 0$, $\gamma_1 f_1 > 0$ and $\gamma_2 p_2 < 0$, $\gamma_2 f_2 < 0$. If $p > \frac{1}{2}$, the dominant process is the transition $|e\rangle \rightarrow |g\rangle$, and $\gamma_2 f_2 > 0$. As it is shown in Table I, f_2 and $\mathcal{P}^g(t)$ change their signs during the time evolution. The purity subflow $\gamma_1 p_1 > 0$ when $\gamma_1 f_1 > 0$. If $p = \frac{1}{2}$, $d\mathcal{P}^g/dt < 0$, with $p_1 > 0$ and $p_2 < 0$; $f_2 = 0$, therefore, there is only one QFI subflow, $\gamma_1 f_1 > 0$.

The phenomena are inverted if the qubit is initialized in the excited state $\rho(0) = |e\rangle\langle e|$. With $r_x = r_y = 0$ and $r_z = 1$, the Bloch vector (32) becomes $\vec{r}(t) = (0, 0, 2\gamma(p-1) + 1)$, and $r_3^e = 2\gamma(p-1) + 1$. All the significant quantities can be obtained by replacing r_3^g with r_3^e , and p with $1-p$ in Eqs. (51)–(53):

$$\frac{d\mathcal{P}^e}{dt} = 2\Gamma e^{-\Gamma t} (1-p)[2\gamma(1-p) - 1], \quad (54)$$

$$F_p^e(t) = \frac{4\gamma^2}{1 - (r_3^e)^2}, \quad (55)$$

$$\frac{dF_p^e}{dt} = \frac{16(1-p)\Gamma\gamma^2(1-\gamma)}{[1 - (r_3^e)^2]^2} \geq 0. \quad (56)$$

C. Observations

To summarize, in the master equation (34), the decoherence rates γ_1 and γ_2 are proportional to $1-p$ and p , respectively. The parameter p to be estimated is the occurrence probability of one of the two opposite processes directing the qubit dynamics, the other process occurring with the probability $1-p$. Therefore, the “ γ_i subflows” associated to F_p dynamics, and those associated to the purity dynamics, have informational contents directly related to the estimated parameter p .

The GAD channel being nonunital (unless $p = \frac{1}{2}$), the qubit purity can increase or decrease during the time evolution, depending on the initial state. The purity subflows $\gamma_1 p_1$ and $\gamma_2 p_2$ have always opposite signs, reflecting their rela-

tion with the occurrence of the opposite processes $|g\rangle \rightarrow |e\rangle$ (probability $1 - p$) and $|e\rangle \rightarrow |g\rangle$ (probability p).

For all initial states considered, the QFI flow associated with the estimation of p is positive, $dF_p/dt > 0$. The increase of the QFI F_p in this Markovian dynamics is due to the fact that the CPTP map depends on p . Since p is a parameter which characterizes the interaction between the qubit and the thermal bath, the qubit can be seen as a quantum probe which efficiently extracts information about the environment (principle of qubit thermometry). The positivity of the QFI flow is reflected in the signs of its subflows. In the decomposition $dF_p/dt = \gamma_1 f_1 + \gamma_2 f_2$, at least one of the subflows is positive. There is a close connection between $d\mathcal{P}/dt$ subflows and dF_p/dt subflows, the positive subflow of the purity being accompanied by a positive subflow of the QFI related to the same decoherence rate.

In short, GAD channel offers a revealing example of Markovian dynamics with a positive dF_p/dt flow, in which the positive and negative QFI subflows reflect the influence of the competing processes in increasing the estimation of p .

IV. QFI DYNAMICS IN THE NON-MARKOVIAN EVOLUTION OF THE ELECTRONIC SUBSYSTEM IN A MOLECULE

We shall now analyze the dynamics of the QFI for a parameter of the electronic subsystem in a molecule. The QFI flow and its subflows will be observed in their connections to the non-Markovian evolution of the electronic subsystem in the vibrational environment of the molecule [42].

We consider a diatomic molecule described in the Born-Oppenheimer (BO) approximation [51], neglecting the rotational degree of freedom, such that the molecule can be described in the bipartite Hilbert space $\mathcal{H} = \mathcal{H}_{el} \otimes \mathcal{H}_{vib}$, which is a tensor product of the electronic and vibrational Hilbert spaces. We suppose that the molecular system is prepared in a pure entangled state $\rho_{el,vib}(t) = |\Psi_{el,vib}(t)\rangle\langle\Psi_{el,vib}(t)|$ of the bipartite system (el \otimes vib), such that N_v vibrational levels of two electronic states (g, e) are populated, therefore, the bipartite Hilbert space has the dimension $2 \times N_v$. In a previous paper [42], we have shown that the evolution of the electronic subsystem in the vibrational environment has a non-Markovian character, correlated to the evolution of the electronic coherence and with the electronic-vibrational entanglement dynamics [52,53].

The matrix of the reduced electronic density $\rho_{el} = \text{Tr}_{vib}(\rho_{el,vib})$ in the electronic basis $\{|g\rangle, |e\rangle\}$ is [42]

$$(\rho_{el})_{\{g,e\}} = \begin{pmatrix} P_g & \langle\psi_e|\psi_g\rangle \\ \langle\psi_g|\psi_e\rangle & P_e \end{pmatrix}, \quad (57)$$

where $|\psi_{g,e}(R, t)\rangle$ are the vibrational wave packets (depending on the internuclear distance R and on the time t) corresponding to the electronic states $|g\rangle, |e\rangle$. P_g and P_e are the populations of the electronic states,

$$P_{g,e}(t) = \langle\psi_{g,e}(R, t)|\psi_{g,e}(R, t)\rangle, \quad (58)$$

obeying the normalization condition $P_g(t) + P_e(t) = 1$. The implicit supposition is that both electronic states g, e are populated: $P_g \neq 0, P_e \neq 0$. The complex overlap of the vibrational

packets can be written as

$$\langle\psi_g|\psi_e\rangle = C(t)e^{i\alpha(t)}, \quad (59)$$

with

$$C(t) = |\langle\psi_g(R, t)|\psi_e(R, t)\rangle|, \quad (60)$$

related to the l_1 norm measure of the electronic coherence [53], $C_{l_1}(\rho_{el}) = 2C(t)$, and $\alpha(t)$ a real function.

The canonical form of the electronic master equation derived in Ref. [42] shows that the evolution of the reduced electronic density $\rho_{el}(t)$ has an inherent non-Markovian character, with one decoherence rate always negative. Here we suppose a molecule with constant electronic populations $P_{g,e}$ in the electronic states g, e (a molecule after the action of a laser pulse, for example, and with no other radial nonadiabatic coupling between the electronic states). We shall consider the QFI associated to the electronic population P_g .

For constant electronic populations $P_{g,e}$ in the electronic states, the master equation describing the non-Markovian evolution of the electronic subsystem in the vibrational environment is [42]

$$\frac{d\rho_{el}}{dt} = \sum_{i=1}^2 \gamma_i(t) \left[A_i(t) \rho_{el} A_i^\dagger(t) - \frac{1}{2} \{A_i^\dagger(t) A_i(t), \rho_{el}\} \right]. \quad (61)$$

The decoherence rates $\{\gamma_i(t)\}_{i=1,2}$, with $\gamma_1 > 0, \gamma_2 < 0$, and $\gamma_2 = -\gamma_1$, have the expressions [42]

$$\gamma_{1,2}(t) = \pm \frac{1}{|\langle\psi_g|\psi_e\rangle|} \left| \frac{d\langle\psi_g|\psi_e\rangle}{dt} \right| \quad (62)$$

$$= \pm \sqrt{\left(\frac{1}{C} \frac{dC}{dt} \right)^2 + \left(\frac{d\alpha}{dt} \right)^2}. \quad (63)$$

The time-dependent decoherence operators $\{A_i(t)\}_{i=1,2}$ are [42]

$$A_1(t) = \frac{n_1}{\sqrt{2}} \left(\sigma_1 + \frac{\gamma_1 - D_{11}}{D_{12}} \sigma_2 \right), \quad (64)$$

$$A_2(t) = \frac{n_2}{\sqrt{2}} \left(\sigma_1 + \frac{\gamma_2 - D_{11}}{D_{12}} \sigma_2 \right), \quad (65)$$

where σ_1, σ_2 are the Pauli operators $\sigma_1 = |e\rangle\langle g| + |g\rangle\langle e|, \sigma_2 = -i|e\rangle\langle g| + i|g\rangle\langle e|$, and n_1, n_2 are real normalization factors (with $n_1^2 + n_2^2 = 1$):

$$n_1^2 = \frac{\gamma_1 - D_{22}}{\gamma_1 - \gamma_2}; \quad n_2^2 = \frac{D_{22} - \gamma_2}{\gamma_1 - \gamma_2}. \quad (66)$$

D_{11}, D_{22} , and D_{12} are the elements of the Hermitian decoherence matrix \mathbf{D} [42]:

$$D_{11}(t) = \frac{1}{2i\hbar} \left[\frac{B(t)}{\langle\psi_g|\psi_e\rangle} - \frac{B^*(t)}{\langle\psi_e|\psi_g\rangle} \right], \quad (67)$$

$$D_{12}(t) = -\frac{1}{2\hbar} \left[\frac{B(t)}{\langle\psi_g|\psi_e\rangle} + \frac{B^*(t)}{\langle\psi_e|\psi_g\rangle} \right], \quad (68)$$

$$D_{22}(t) = -\frac{1}{2i\hbar} \left[\frac{B(t)}{\langle\psi_g|\psi_e\rangle} - \frac{B^*(t)}{\langle\psi_e|\psi_g\rangle} \right], \quad (69)$$

with $B(t) = i\hbar(d\langle\psi_e|\psi_g\rangle/dt)$. As D_{11}, D_{22} , and D_{12} are real, the decoherence operators A_i are Hermitian, and $[A_i, A_i^\dagger] = 0$.

Let us consider the QFI F_{P_g} associated to the parameter P_g , the electronic population in one of the two electronic states. The decoherence rates $\gamma_i(t)$ [Eq. (63)] and the decoherence operators $A_i(t)$ [Eqs. (64) and (65)] depend on the coherence $C(t)$ [Eq. (60)], which depends on P_g [Eq. (58)]: $\frac{\partial C}{\partial P_g} \neq 0$. Therefore, $\gamma_i(t)$ and $A_i(t)$ depend on the parameter P_g :

$$\frac{\partial \gamma_i}{\partial P_g} \neq 0, \quad \frac{\partial A_i}{\partial P_g} \neq 0. \quad (70)$$

The dynamical behavior of $F_{P_g}(t)$ will be analyzed using the equations established in Sec. II. The electronic density operator $\rho_{el}(t)$ can be written in the Bloch representation (6), with the Bloch vector

$$\vec{\omega}(t) = (2C(t) \cos \alpha(t), -2C(t) \sin \alpha(t), 1 - 2P_g). \quad (71)$$

The QFI F_{P_g} depends on the partial derivative

$$\frac{\partial \vec{\omega}}{\partial P_g} = \left(2 \frac{\partial C}{\partial P_g} \cos \alpha, -2 \frac{\partial C}{\partial P_g} \sin \alpha, -2 \right). \quad (72)$$

Equation (11) gives the following formulas for the quantities a and \vec{b} associated to the calculation of the QFI F_{P_g} :

$$a = -\frac{1}{L} \left[\frac{\partial C^2}{\partial P_g} + P_g - P_e \right] = \frac{1}{2L} \frac{\partial L}{\partial P_g}, \quad (73)$$

$$\vec{b} = -a\vec{\omega} + \partial_{P_g}\vec{\omega}, \quad (74)$$

where L is the linear entropy $L(t) = 1 - \text{Tr}[\rho_{el}^2(t)]$ of the electronic-vibrational entanglement, given by [52]

$$L(t) = 2P_gP_e - 2C^2(t). \quad (75)$$

The purity of the electronic subsystem is

$$\mathcal{P}(t) = 1 - L(t) = P_g^2 + P_e^2 + 2C^2(t). \quad (76)$$

Using Eq. (9) one obtains the QFI F_{P_g} as

$$F_{P_g} = 4 + 4 \left(\frac{\partial C}{\partial P_g} \right)^2 + \frac{2}{L} \left(\frac{\partial C^2}{\partial P_g} + P_g - P_e \right)^2 \quad (77)$$

$$= 4 + 4 \left(\frac{\partial C}{\partial P_g} \right)^2 + \frac{1}{2L} \left(\frac{\partial L}{\partial P_g} \right)^2. \quad (78)$$

Equation (77) shows that $F_{P_g} = F_{P_e}$ and $F_{P_g} > 4$. The time behavior of F_{P_g} is determined by the coherence C and its partial derivative $\partial C/\partial P_g$.

A. $d\mathcal{P}/dt$ decomposition into γ_i subflows

The time derivative of the purity [Eq. (76)]

$$\frac{d\mathcal{P}}{dt} = 4C \frac{dC}{dt} \quad (79)$$

can be decomposed into subflows using Eq. (23) as

$$\frac{d\mathcal{P}}{dt} = -2 \sum_i \gamma_i q'_i, \quad (80)$$

with $q'_i \geq 0$. Therefore, $d\mathcal{P}/dt$ can be seen as the sum of two subflows, one negative corresponding to the positive decoherence rate γ_1 , and one positive corresponding to the negative decoherence rate γ_2 .

B. dF_{P_g}/dt decomposition into subflows and the canonical measure of non-Markovianity

We shall use Eq. (25) to analyze the QFI dynamics in relation to the decoherence rates. Taking into account that $\sum_i \gamma_i = 0$, $A_i = A_i^+$, and $H = 0$, dF_{P_g}/dt has the structure

$$\frac{dF_{P_g}}{dt} = -a \sum_{i=1,2} \gamma_i \text{Tr}[A_i \vec{\omega} \cdot \vec{\sigma} A_i \vec{b} \cdot \vec{\sigma}] + 2\vec{b} \cdot \frac{d}{dt} \left(\frac{\partial \vec{\omega}}{\partial P_g} \right), \quad (81)$$

with three terms $dF_{P_g}/dt = T_1 + T_2 + T_3$. The first two terms are the subflows T_i ($i = 1, 2$) corresponding to the decoherence rates γ_i , and the third term T_3 is a subflow introducing the second derivative $\frac{d}{dt} \left(\frac{\partial C}{\partial P_g} \right)$. Using Eqs. (64), (65), (73), and (74), we obtain

$$T_i = -a\gamma_i \text{Tr}[A_i \vec{\omega} \cdot \vec{\sigma} A_i \vec{b} \cdot \vec{\sigma}] \quad (82)$$

$$= -\{[a(P_e - P_g) + 1]^2 - 1\} \gamma_i + 4a \left(aC - \frac{\partial C}{\partial P_g} \right) \frac{dC}{dt}, \quad (83)$$

$$T_3 = 2\vec{b} \cdot \frac{d}{dt} \left(\frac{\partial \vec{\omega}}{\partial P_g} \right) = -8 \left(aC - \frac{\partial C}{\partial P_g} \right) \frac{d}{dt} \left(\frac{\partial C}{\partial P_g} \right). \quad (84)$$

Let us remark that, on the right side of Eq. (83), $-\gamma_i$ is multiplied by the factor $[a(P_e - P_g) + 1]^2 - 1$, which is positive if $a(P_e - P_g) > 0$; it can be shown that this condition is fulfilled if

$$\left| \frac{\partial C^2}{\partial P_g} \right| < |P_e - P_g|. \quad (85)$$

In its compact form, the QFI flow is an oscillating function determined by the behavior of the coherence and its various derivatives:

$$\frac{dF_{P_g}}{dt} = 8 \left(aC - \frac{\partial C}{\partial P_g} \right) \left[a \frac{dC}{dt} - \frac{d}{dt} \left(\frac{\partial C}{\partial P_g} \right) \right], \quad (86)$$

with a given in Eq. (73). Equation (86) can be rewritten as

$$\frac{dF_{P_g}}{dt} = \frac{8F^2}{L^2} \left(\frac{1}{C} \frac{dC}{dt} \right) - \frac{8CF}{L} \frac{\partial}{\partial P_g} \left(\frac{1}{C} \frac{dC}{dt} \right), \quad (87)$$

where we have used the notation $F = C(P_e - P_g) - 2P_gP_e \frac{\partial C}{\partial P_g}$.

On the other hand, the canonical measure of non-Markovianity [37,42] is defined in relation to the negative canonical decoherence rate $\gamma_2(t)$, as the function $f(t) = |\gamma_2(t)|$. Using Eq. (63), one obtains

$$f(t) = \sqrt{\left(\frac{1}{C} \frac{dC}{dt} \right)^2 + \left(\frac{d\alpha}{dt} \right)^2} \sim \left| \frac{1}{C} \frac{dC}{dt} \right|. \quad (88)$$

Equations (87) and (88) show that the QFI flow dF_{P_g}/dt and the non-Markovianity measure $f(t)$ are both determined by the temporal behavior of the electronic coherence, through $\frac{1}{C} \frac{dC}{dt}$.

In the following, we shall analyze on a numerical example the QFI flow dF_{P_g}/dt and its decomposition into subflows, in relation to the time evolutions of the coherence $C(P_g, t)$ and of the non-Markovianity measure $f(t)$.

C. Electronic populations, electronic coherence, and the partial derivative $\frac{\partial C}{\partial P_g}$

The QFI F_{P_g} [Eq. (77)] is determined by the partial derivative of the electronic coherence $C(P_g, t)$ relative to the parameter P_g , $\frac{\partial C}{\partial P_g}$. We shall precise the character of this dependence. Previous works [52,53] contain more detailed descriptions of the molecular model of a diatomic molecule in the Born-Oppenheimer (BO) approximation [51]. The nuclear motion in an electronic state $|\alpha\rangle$ is determined by the corresponding electronic potential $V_\alpha(R)$. If T_R is the nuclear kinetic energy operator, the Schrödinger equation giving the vibrational eigenfunctions $|\chi_{v_\alpha}(R)\rangle$ and vibrational energies E_{v_α} is

$$[T_R + V_\alpha(R)]|\chi_{v_\alpha}(R)\rangle = E_{v_\alpha}|\chi_{v_\alpha}(R)\rangle. \quad (89)$$

The eigenvectors $\{|\chi_{v_\alpha}(R)\rangle\}_{v_\alpha=1, \dots, N_\alpha}$ form an orthonormal vibrational basis with dimension N_α corresponding to the electronic surface α . The vibrational wave packet corresponding to the electronic potential α can be developed in this basis as

$$|\psi_\alpha(R, t)\rangle = \sum_{v_\alpha=1}^{N_\alpha} c_{v_\alpha}(t)|\chi_{v_\alpha}(R)\rangle, \quad (90)$$

with the complex coefficient $c_{v_\alpha}(t)$ providing the probability $|c_{v_\alpha}(t)|^2$ for the population of the vibrational state $|\chi_{v_\alpha}(R)\rangle$.

In a molecule with two uncoupled electronic channels $\alpha = g, e$, each vibrational wave packet $|\psi_\alpha(R, t)\rangle$ evolves in the corresponding electronic potential $V_\alpha(R)$ according to the time-dependent Schrödinger equation $[T_R + V_\alpha(R)]|\psi_\alpha(R, t)\rangle = i\hbar\partial/\partial t|\psi_\alpha(R, t)\rangle$. Therefore, the probability amplitude $c_{v_\alpha}(t)$ is

$$c_{v_\alpha}(t) = c_{v_\alpha}(t_i)e^{-\frac{i}{\hbar}E_{v_\alpha}(t-t_i)}, \quad (91)$$

where t_i is a time moment after which the electronic channels can be considered uncoupled (after being coupled by a laser pulse which populates the electronic states, for example), and E_{v_α} is the vibrational energy corresponding to the vibrational function $|\chi_{v_\alpha}(R)\rangle$. Therefore, the population of the electronic state $P_g = \langle\psi_g|\psi_g\rangle$ is

$$P_g = \sum_{v_g} |c_{v_g}(t_i)|^2, \quad (92)$$

and the square of the coherence $C(t)$ can be written

$$\begin{aligned} C^2 &= |\langle\psi_g(R, t)|\psi_e(R, t)\rangle|^2 \\ &= \sum_{v_g, v'_g} \sum_{v_e, v'_e} c_{v_g}^*(t_i)c_{v_e}(t_i)c_{v'_g}(t_i)c_{v'_e}^*(t_i) \\ &\quad \times \mathcal{F}_{v_g v_e} \mathcal{F}_{v'_g v'_e}^* e^{\frac{i}{\hbar}[(E_{v_g} - E_{v'_g}) - (E_{v_e} - E_{v'_e})](t-t_i)}, \end{aligned} \quad (93)$$

with $\mathcal{F}_{v_g v_e} = \langle\chi_{v_g}(R)|\chi_{v_e}(R)\rangle$ the overlap integral of two vibrational wave functions. The coherence dependence on the electronic populations is intricate, as it can be seen from Eq. (93), showing that $C(t)$ implies summations of the vibronic coherences $c_{v'_g}^*(t_i)c_{v_e}(t_i)$ coming from all the populated vibrational levels [53].

1. Connections with the vibrational environment

Let us observe that the probability amplitudes $c_{v_g}(t)$, $c_{v_e}(t)$, which determine the electronic populations, the vibronic coherences, and the electronic coherence, are also related to the matrix elements of $\rho_{\text{vib}} = \text{Tr}_{\text{el}}(\rho_{\text{el, vib}})$, the reduced density operator of the vibrational environment. The pure entangled state of the molecular system being $|\Psi_{\text{el, vib}}(t)\rangle = |g\rangle \otimes |\psi_g(t)\rangle + |e\rangle \otimes |\psi_e(t)\rangle$ [52], one obtains $\rho_{\text{vib}} = |\psi_g\rangle\langle\psi_g| + |\psi_e\rangle\langle\psi_e|$. In an orthonormal basis $\{|u_n\rangle\}_{n=1, \dots, N_v}$ of the vibrational Hilbert space \mathcal{H}_{vib} , the populations of ρ_{vib} are

$$\begin{aligned} \langle u_n | \rho_{\text{vib}} | u_n \rangle &= \sum_{v_g, v'_g} c_{v_g} c_{v'_g}^* \langle \chi_{v'_g}(R) | u_n \rangle \langle u_n | \chi_{v_g}(R) \rangle \\ &\quad + \sum_{v_e, v'_e} c_{v_e} c_{v'_e}^* \langle \chi_{v'_e}(R) | u_n \rangle \langle u_n | \chi_{v_e}(R) \rangle. \end{aligned} \quad (94)$$

A similar formula gives the coherences $\langle u_n | \rho_{\text{vib}} | u_m \rangle$. Equation (94) shows the way in which the information about the electronic population (P_g or P_e) is structurally encoded in the vibrational environment.

2. 2×2 molecular system: One vibrational level in each electronic state

We shall now refer to examples which allow to find simple analytical formulas for $\frac{\partial C}{\partial P_g}$. We shall suppose only one vibrational level populated in the ground electronic state. We begin with the simple example of a 2×2 system, and afterwards we shall discuss $2 \times N_v$ molecular systems.

Let us suppose one vibrational level populated in each electronic state, namely, v_g in the electronic state g and v_e in the electronic state e . Therefore, $P_g = |c_{v_g}|^2$, $P_e = |c_{v_e}|^2$, $P_g + P_e = 1$. Equation (93) gives the coherence

$$C = \sqrt{P_g(1 - P_g)} |\mathcal{F}_{v_g v_e}|, \quad (95)$$

which does not vary in time, $dC/dt = 0$. With Eqs. (63) and (59) the decoherence rates $\{\gamma_i\}_{i=1,2}$ become

$$\gamma_{1,2} = \pm \frac{|E_{v_g} - E_{v_e}|}{\hbar}. \quad (96)$$

Using Eqs. (95) and (77) one obtains the QFI

$$F_{P_g} = \frac{1}{P_g P_e}, \quad (97)$$

constant in time, $dF_{P_g}/dt = 0$. Equations (81), (83), and (84) show dF_{P_g}/dt as the result of two opposite subflows corresponding to the decoherence rates, a positive subflow $-a^2\gamma_2$ for $\gamma_2 < 0$, and a negative subflow $-a^2\gamma_1$ for $\gamma_1 > 0$,³ which cancel each other out:

$$\frac{dF_{P_g}}{dt} = -a^2\gamma_1 - a^2\gamma_2 = 0, \quad (98)$$

with $a = (P_e - P_g)(1 - |\mathcal{F}_{v_g v_e}|^2)/L$.

³The condition (85) is fulfilled in this case, with $|\partial C^2/\partial P_g| = |P_e - P_g| |\mathcal{F}_{v_g v_e}|^2 < |P_e - P_g|$.

3. $2 \times N_v$ system: One vibrational level in the electronic state g and $N_v - 1$ vibrational levels in the electronic state e

Let us consider one vibrational level v_g populated in the electronic state g and $N_v - 1$ vibrational levels $\{v_e\}$ populated in the electronic state e , such that

$$|\psi_g(R, t)\rangle = c_g(t_i) e^{-\frac{i}{\hbar} E_{v_g}(t-t_i)} |\chi_{v_g}(R)\rangle, \quad (99)$$

$$|\psi_e(R, t)\rangle = \sum_{v_e} c_{v_e}(t_i) e^{-\frac{i}{\hbar} E_{v_e}(t-t_i)} |\chi_{v_e}(R)\rangle. \quad (100)$$

The electronic populations are $P_g = |c_g(t_i)|^2$ and $P_e = \sum_{v_e} |c_{v_e}(t_i)|^2$, with $P_g + P_e = 1$.

Writing the complex amplitudes as $c_{v_{e_i}}(t_i) = |c_{v_{e_i}}| e^{i e_i}$, and the overlap integral $\mathcal{F}_{v_g v_{e_i}}$ between the ground vibrational wave function v_g and an excited vibrational wave function v_{e_i} as $\mathcal{F}_{v_g v_{e_i}} = |\mathcal{F}_{v_g v_{e_i}}| e^{i f_i}$, Eq. (93) gives

$$C^2(P_g, t) = P_g \left(\sum_{v_e} |c_{v_e}|^2 |\mathcal{F}_{v_g v_e}|^2 + 2 \sum_{v_{e_i}} \sum_{v_{e_j} \neq v_{e_i}} |c_{v_{e_i}}| |c_{v_{e_j}}| |\mathcal{F}_{v_g v_{e_i}}| |\mathcal{F}_{v_g v_{e_j}}| \mathcal{A}_{ij}(t) \right). \quad (101)$$

The temporal behavior of $C^2(P_g, t)$ is shaped by the various $\mathcal{A}_{ij}(t) = \cos[a_{ij} + \omega_{v_{e_j} v_{e_i}}(t - t_i)]$, with $a_{ij} = e_i - e_j + f_i - f_j$ a phase depending on the quantum molecular preparation at t_i , and $\omega_{v_{e_j} v_{e_i}} = (E_{v_{e_j}} - E_{v_{e_i}})/\hbar$. For example, if there are only two neighboring vibrational levels v_e and $v_e + 1$ populated in the excited electronic state e , $\mathcal{A}_{12}(t)$ and $C^2(t)$ oscillate with a characteristic time which is the vibrational period of v_e : $T_{\text{vib}}(v_e) = 2\pi\hbar/|E_{v_e+1} - E_{v_e}|$ [54].

The partial derivative $\frac{\partial C^2}{\partial P_g} = 2C \frac{\partial C}{\partial P_g}$ can be deduced from Eq. (101) taking into account that $\sum_{v_e} |c_{v_e}|^2 = 1 - P_g$. Finally, we find

$$\frac{\partial C}{\partial P_g} = \frac{C}{2P_g} - \frac{P_g}{2C} \left[\sum_{v_e} |\mathcal{F}_{v_g v_e}|^2 + \sum_{v_{e_i}} \sum_{v_{e_j} \neq v_{e_i}} |\mathcal{F}_{v_g v_{e_i}}| |\mathcal{F}_{v_g v_{e_j}}| \frac{|c_{v_{e_i}}|^2 + |c_{v_{e_j}}|^2}{|c_{v_{e_i}}| |c_{v_{e_j}}|} \mathcal{A}_{ij}(t) \right]. \quad (102)$$

D. Example: $F_{P_g}(t)$ dynamics in a molecule with two electronic states and mainly five populated vibrational levels

We will take as example a quantum preparation of the Cs_2 molecule, which is obtained by simulating the action of a chirped laser pulse, chosen such that mainly five vibrational levels are populated in the electronic states $a^3\Sigma_u^+(6s, 6s)$ and $1_g(6s, 6p_{3/2})$: the level $v_g = 0$ of the ground state $g = a^3\Sigma_u^+$, and the vibrational levels $v_e = 2, 3, 4, 5$ of the excited state $e = 1_g$ (see Fig. 1).

Quantum preparations of this type were analyzed in Ref. [53], where various chirped pulses were used to simulate molecular preparations with different electronic-nuclear

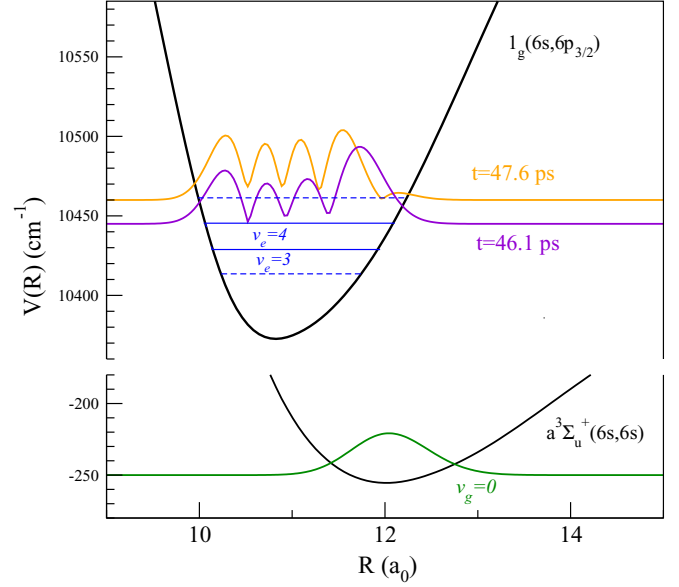


FIG. 1. $a^3\Sigma_u^+(6s, 6s)$ and $1_g(6s, 6p_{3/2})$ electronic potentials of Cs_2 (the energy origin is the dissociation limit $E_{6s+6s} = 0$ of the $a^3\Sigma_u^+$ potential). Picture of a molecular preparation with mainly five populated vibrational levels, $v_g = 0$ of the $a^3\Sigma_u^+$ potential and $v_e = 2, 3, 4, 5$ of the 1_g electronic potential. The excited vibrational wave packet $|\psi_e(R, t)\rangle$ in the 1_g potential is shown at $t = 46.1$ ps (coherence maximum) and 47.6 ps (coherence minimum).

entanglement dynamics. The theoretical model and numerical techniques were described in previous works [52,53,55]. The chirped pulse [56] is represented by an electric field $\mathcal{E}(t) = \mathcal{E}_0 e(t) \cos[\omega_L t + \varphi(t)]$, with amplitude \mathcal{E}_0 , Gaussian temporal envelope $e(t) = \sqrt{\tau_L/\tau_C} \exp\{-2 \ln 2[(t - t_p)/\tau_C]^2\}$ is centered at $t = t_p$ and has the temporal width τ_C , with its maximum determined by $\tau_L/\tau_C \leq 1$, τ_L being the temporal width of the pulse before chirping. The multitude of the parameters characterizing a chirped pulse allows various possibilities to control the molecular preparations [55,57].

We describe briefly the choice of the pulse parameters allowing to obtain the molecular preparation sketched in Fig. 1. We have used a chirped pulse with central energy $\hbar\omega_L = 10695 \text{ cm}^{-1}$ to couple the electronic potentials $a^3\Sigma_u^+$ and 1_g at the internuclear distance $R_c \approx 12 a_0$, transferring population from the ground state $v_g = 0$ of $g = a^3\Sigma_u^+$ to the excited state $e = 1_g$ (see Fig. 1). The pulse parameters are $t_p = 15$ ps, $\tau_L = 0.6$ ps, a positive chirp rate $\chi = 3.33 \text{ ps}^{-2}$, and $\tau_C = 1.7$ ps. The strength coupling $W_L = \mathcal{E}_0 D_{ge}/2$, a function of the laser intensity I ($\mathcal{E}_0 = \sqrt{2I/c\epsilon_0}$) and the transition dipole moment D_{ge} between the electronic surfaces [58], is chosen $W_L = 10.97 \text{ cm}^{-1}$.

Here we refer only to the vibrational dynamics after pulse, when the electronic populations remain constant in time. The dynamics of the vibrational wave packets $\psi_{g,e}(R, t)$ in the electronic channels is obtained by propagating in time the wave packets on a spatial grid with length L_R , using the

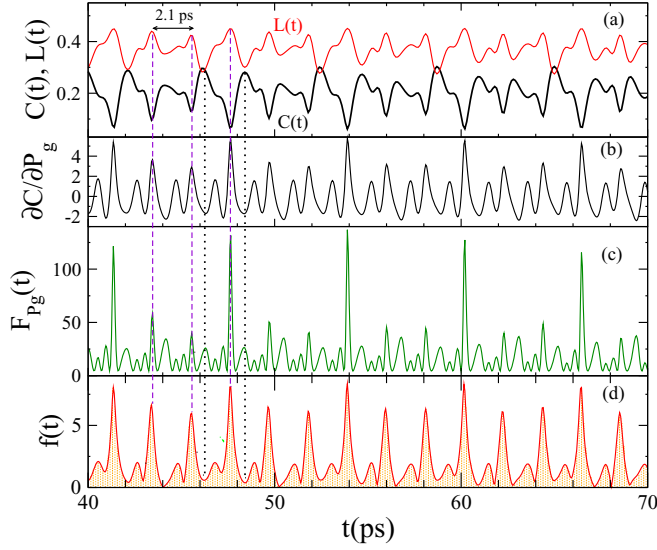


FIG. 2. (a) Time evolution of the electronic coherence $C(t)$ and linear entropy $L(t)$. (b) Time evolution of the partial derivative $\frac{\partial C}{\partial P_g}$. (c) Time evolution of the QFI $F_{P_g}(t)$. (d) Non-Markovianity measure $f(t)$. The filled surface shows the integral $\int f(t)dt$. The dashed vertical lines and the dotted vertical lines correspond to minima and maxima of the electronic coherence $C(t)$, respectively.

Chebyshev expansion of the evolution operator [59,60] and the mapped sine grid (MSG) method [55,61] to represent the radial dependence of the wave packets. The electronic populations and the electronic coherence are calculated from the vibrational wave packets as $P_{g,e}(t) = \int_0^{L_R} |\Psi_{g,e}(R', t)|^2 dR'$ and $C(t) = \int_0^{L_R} \Psi_g^*(R', t) \Psi_e(R', t) dR'$, respectively. The coherence $C(t)$ can be chosen as the reference dynamical quantity because its temporal behavior underlies the dynamics of the other significant quantities, such as the electronic purity [Eq. (76)] or the linear entropy measuring the electronic-vibrational entanglement. The local minima (maxima) of the coherence $C(t)$ are local minima (maxima) of the purity $\mathcal{P}(t)$ and maxima (minima) of the entanglement measured by $L(t)$.

After pulse, the electronic population is distributed between $g = a^3 \Sigma_u^+$ and $e = 1_g$, with $v_g = 0$ populated in the ground state g and mainly $v_e = 2, 3, 4, 5$ populated in the excited state e . The time evolutions of the coherence $C(t)$ and linear entropy $L(t)$ after pulse are shown in Fig. 2(a). They exhibit oscillations with the characteristic periods expected from Eq. (101). Indeed, the vibrational levels $v_e = 2, 3, 4, 5$ of the electronic state 1_g are separated by an energy gap of $\approx 16 \text{ cm}^{-1}$ (corresponding to a vibrational period of about 2 ps), therefore, three characteristic periods are expected to appear in the time oscillations of the electronic coherence and linear entropy, corresponding to the various frequencies $\omega_{v_e, v_{e_i}}$: mainly 2.1 ps, but also 1.04 and 0.7 ps.

We have used Eq. (102) to calculate the partial derivative $\frac{\partial C}{\partial P_g}$ after pulse, taking $t_i = 20 \text{ ps}$. Let us observe [Figs. 2(a) and 2(b), and Eq. (102)] that the local maxima of the function $\frac{\partial C}{\partial P_g}(t)$ appear when $C(t)$ has local minima. Figures 2(a)–2(d) illustrate the time evolution of $F_{P_g}(t)$ [Eq. (77)] in relation to the coherence $C(t)$, the linear entropy $L(t)$, the partial deriva-

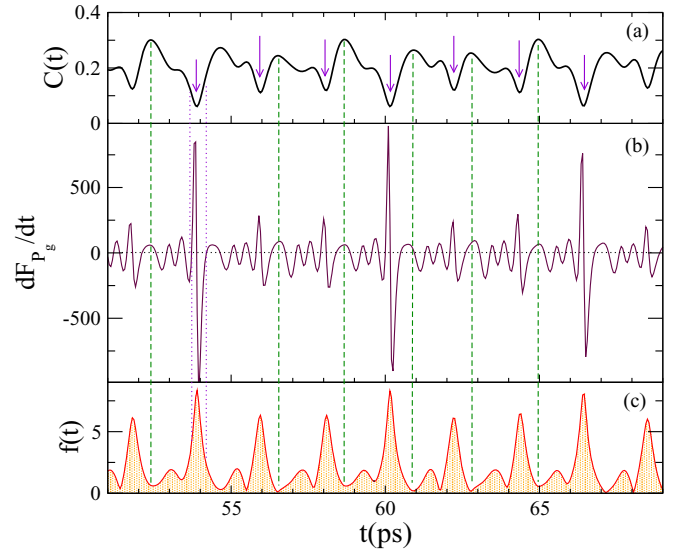


FIG. 3. The QFI flow dF_{P_g}/dt in relation to the electronic coherence $C(t)$ and the non-Markovianity measure $f(t)$. (a) Time evolution of the electronic coherence $C(t)$. (b) Time evolution of the QFI derivative dF_{P_g}/dt . (c) Canonical non-Markovianity measure $f(t)$. The dotted vertical lines marks the change of the QFI flow dF_{P_g}/dt from a sharp positive maximum to a sharp negative minimum when the electronic coherence $C(t)$ reaches a minimum. The dashed vertical lines correspond to maxima of $C(t)$.

tive $\frac{\partial C}{\partial P_g}(t)$, and the non-Markovianity measure $f(t)$ [Eq. (88)]. It can be seen that the minima of the coherence $C(t)$ [entanglement maxima of $L(t)$] correspond to sharp maxima in the evolution of $F_{P_g}(t)$, and to maxima in the time evolution of the non-Markovianity measure $f(t)$ (see the vertical dashed lines on the figures). On the contrary, the coherence local maxima correspond to smaller local maxima of $F_{P_g}(t)$ and to minima of the non-Markovianity measure $f(t)$ (vertical dotted lines on the figures). A similar observation can be made on Figs. 3(a)–3(c) which depict the QFI flow dF_{P_g}/dt in relation to the electronic coherence and the non-Markovianity measure. It can be observed that diminution of the coherence $C(t)$ to a minimum and its subsequent increase corresponds to a sudden change of the QFI flow dF_{P_g}/dt from sharp positive to sharp negative values. On the contrary, around the local maxima of the coherence the QFI flow is rather positive. The non-Markovianity maxima of $f(t)$ correspond to maxima of the QFI $F_{P_g}(t)$ and to the sudden change of sign of the QFI flow: $dF_{P_g}/dt > 0$ when $f(t)$ increases, and $dF_{P_g}/dt < 0$ when $f(t)$ decreases [see the vertical lines on Figs. 3(a)–3(c)].

Figures 4 and 5 depict the subflows $T_i(t)$ ($i = 1, 2, 3$) corresponding to the decomposition $dF_{P_g}/dt = T_1(t) + T_2(t) + T_3(t)$ [Eqs. (83) and (84)]. Figures 4(a) and 4(b) show the QFI subflows $T_1(t)$ and $T_2(t)$ corresponding to the decoherence rates $\gamma_1(t) > 0$ and $\gamma_2(t) < 0$, respectively. Both subflows oscillate taking positive and negative values. During the time intervals with significant non-Markovianity [maxima of $f(t) = |\gamma_2(t)| = \gamma_1(t)$], the subflow $T_1(t)$ corresponding to the positive decoherence rate $\gamma_1(t) > 0$ becomes positive, with maxima following the maxima of $\gamma_1(t)$, and hence it

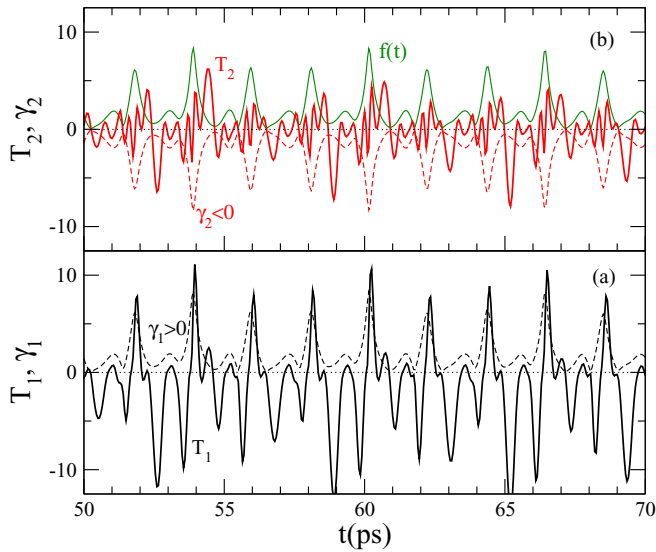


FIG. 4. QFI subflows $T_1(t)$ and $T_2(t)$ corresponding to the decoherence rates $\gamma_1(t) > 0$ and $\gamma_2(t) < 0$, respectively. (a) Time evolution of $T_1(t)$ (full line) and $\gamma_1(t) > 0$ (dashed line). (b) Time evolution of $T_2(t)$ (full line) and $\gamma_2(t) < 0$ (dashed line). The canonical non-Markovianity measure $f(t) = |\gamma_2(t)| = \gamma_1(t)$ (thin line) is shown.

contributes to the increase of the QFI. In the same intervals, the subflow $T_2(t)$, corresponding to $\gamma_2(t) < 0$, strongly oscillates keeping rather positive values. In the time intervals in which $f(t)$ has low values, both subflows $T_1(t)$ and $T_2(t)$ reach large negative values.

Figures 5(a) and 5(b) show the sum $T_1(t) + T_2(t)$ of the subflows related to the decoherence rates, and the third subflow, $T_3(t)$. Figure 5(a) shows that non-Markovianity maxima are accompanied by a positive sum $T_1(t) + T_2(t)$, and that the low values of $f(t)$ are associated to a negative sum of the

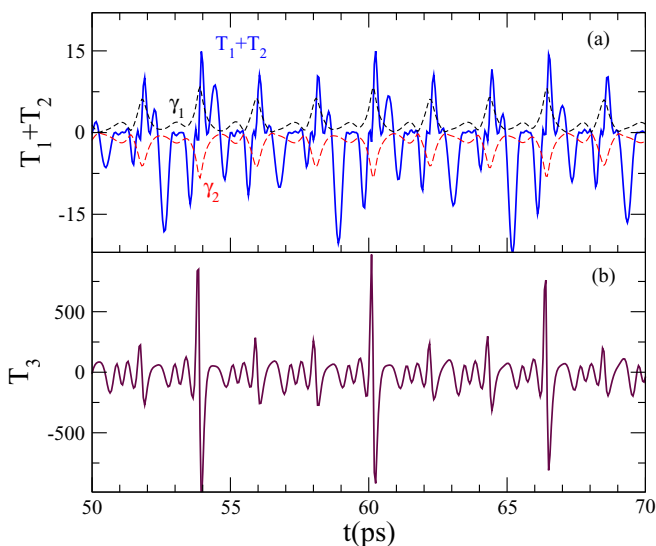


FIG. 5. (a) The sum of the QFI subflows $T_1(t) + T_2(t)$. The decoherence rates $\gamma_1(t) > 0$ and $\gamma_2(t) < 0$ are shown with dashed lines (the canonical non-Markovianity measure $f(t) = |\gamma_2(t)| = \gamma_1(t)$). (b) The QFI subflow $T_3(t)$.

subflows $T_1(t) + T_2(t)$. The subflows $T_1(t)$, $T_2(t)$, as well as their sum $T_1(t) + T_2(t)$, have a very small contribution in the total QFI flow, $|T_1(t) + T_2(t)| \ll |T_3(t)|$, such that the third subflow is the dominant one, $dF_g/dt \approx T_3(t)$.

E. Discussion

This analysis shows that the time behavior of the QFI flow dF_g/dt is strongly connected to the non-Markovian dynamics of the electronic subsystem. Equations (87) and (88) disclose that this connection is rooted in the time behavior of the electronic coherence, a basic quantity in defining the correlations between the electronic open system and its vibrational environment. The positive QFI flow dF_g/dt can be correlated to the increase of the canonical non-Markovianity measure $f(t)$, the increase of electronic-vibrational entanglement $L(t)$, and the decrease of the electronic coherence $C(t)$.

In the dF_g/dt decomposition into subflows, the third subflow, which is not associated to the decoherence rates, is the dominant one. We have shown that all three types of subflows can take positive or negative values, contributing to the increase or decrease of the information about the parameter in the open system. The subflow corresponding to the negative decoherence rate T_2 is the one to be associated to non-Markovianity measured with the canonical measure $f(t) = |\gamma_2(t)|$. T_2 distinguishes by a strong oscillating character when $f(t)$ has large values, acquiring large negative values when non-Markovianity is diminished. On the other hand, in this specific case, the positive decoherence rate $\gamma_1(t) = |\gamma_2(t)| = f(t)$. The subflow T_1 corresponding to $\gamma_1(t)$ appears to take large positive values when $\gamma_1(t)$ reaches maxima, and large negative values when $\gamma_1(t)$ has low values. Therefore, the information on the parameter P_g quantified by $F_g(t)$ can be increased (or decreased) not only by the dynamics corresponding to $\gamma_2 < 0$ (usually associated to information backflow from the environment to the system), but also during the dynamics corresponding to $\gamma_1 > 0$. The fundamental reason is that the information about P_g is structurally contained in the electronic open system, the vibrational environment (see Sec. IV C 1), and in their correlations (coherence, entanglement), being continuously circulated between them during the dynamics.

V. CONCLUSIONS

We have analyzed the dynamics of the QFI $F_\theta(t)$ for a two-dimensional open quantum system which obeys a time-local non-Markovian master equation in the canonical form [37], characterized by decoherence rates $\gamma_i(\theta, t)$, and operators $H(\theta, t)$, $A_i(\theta, t)$, that depend on the parameter θ to be estimated. The dependence of the dynamics on the parameter brings an extended framework, beyond the conditions on the time-local master equation [36] implied in the approach to the QFI flow employed in Ref. [31]. In the present case, the information about θ is structurally encoded not only “inside” the open system, but also “outside,” in the environment and its interaction or/and correlations with the open system. As the dynamical map defining the time evolution of the open system is dependent on the parameter θ , the QFI $F_\theta(t)$ may increase also in Markovian dynamics.

In this extended framework, we have explored the new decomposition of the QFI flow into subflows, and their structural relations to the open system dynamics. The non-Markovianity of the open system dynamics was characterized using the canonical measure $f(\theta, t)$, defined from the occurrence of negative decoherence rates $\gamma_i(\theta, t) < 0$ in the canonical master equation. Because the decoherence rates depend on the parameter, the canonical measure of non-Markovianity $f(\theta, t)$ is a function of θ , and therefore it has an underlying connection with the QFI flow dF_θ/dt .

In Sec. II we have derived analytic formulas expressing the time evolution of the system's purity ($d\mathcal{P}/dt$) and of the QFI flow (dF_θ/dt), in terms associated to the decoherence rates, in a general case, in which the decoherence operators may be non-Hermitian, and the generator of the master equation may be nonunital. The decomposition of $d\mathcal{P}/dt$ allows to distinguish the various contributions to the purity dynamics, for example, those coming from nonunital dynamics, and from the sum of the decoherence rates. In contrast to the results of Ref. [31], we have shown that the QFI flow dF_θ/dt contains not only the subflows associated to the decoherence rates, but also supplementary terms coming from the dependence of the quantum state on the parameter θ . Moreover, the signs of the QFI subflows associated to the decoherence rates cannot be correlated to the signs of the decoherence rates, as it is the case in the decomposition obtained in Ref. [31].

These analytic results were employed to explore the QFI flow and subflows in two cases of open system dynamics: (i) The Markovian nonunital evolution of a qubit under the GAD channel, characterized by a master equation with decoherence rates that depend on the estimated parameter, and then a dynamical map which depends on the estimated parameter. This is a paradigmatic case of Markovian dynamics that can lead to the increase of the QFI. (ii) The non-Markovian evolution of the electronic subsystem in a molecule, as an open system entangled with the vibrational environment. We shall briefly present the main results obtained in these cases.

Section III explored the dynamics of the QFI F_p associated with the parameter p related to the bath temperature, in the Markovian nonunital evolution of a qubit under the GAD channel, for three initial states of the qubit. For all initial states considered, the QFI flow dF_p/dt associated with the estimation of p is positive, showing that the precision of the estimation increases with the interaction time. The QFI growth during the GAD Markovian time evolution is the consequence of the fact that the CPTP map depends on p , a parameter which characterizes the interaction between the qubit and the thermal bath. The qubit acts as a quantum probe which extracts information about the environment, this being its role in qubit thermometry [46,47,62]. The GAD channel is particularly relevant for the decompositions of $d\mathcal{P}/dt$ and dF_p/dt into subflows associated to the decoherence rates because the subflows have clear meanings related to the change of information between the qubit and the thermal bath. The two decoherence rates are proportional to p and $1 - p$, respectively, the probabilities of the opposite processes in which the qubit exchanges energy with the bath. $d\mathcal{P}/dt$ and dF_p/dt can both be written as sum of two subflows proportional to p and $1 - p$, while p is also the parameter to be estimated. Consequently, the subflows have an infor-

mational content directly related to the estimated parameter p , and this content is reflected in their signs during the time evolution.

In Sec. IV we have examined the QFI flow and its subflows in the non-Markovian evolution of a two-dimensional electronic subsystem in the vibrational environment of a molecule described in the bipartite Hilbert space $\mathcal{H} = \mathcal{H}_{el} \otimes \mathcal{H}_{vib}$. In this specific case, the electronic open system and the vibrational environment are entangled, and their correlations are manifested in various dynamic quantities, such as the electronic coherence $C(t)$, the electronic purity, and the linear entropy of the electronic-vibrational entanglement $L(t)$. The parameter P_g is the electronic population in one of the two populated electronic states ($P_g + P_e = 1$). P_g characterizes the electronic reduced state $\rho_{el}(t)$, but the information about P_g is also encoded in the vibrational environment, and in the correlations between system and environment [coherences, linear entropy of the entanglement $L(t)$], through the amplitudes defining the vibronic coherences. $\rho_{el}(t)$ obeys a time-local non-Markovian master equation, with two time-dependent canonical decoherence rates, one positive, the other negative [$\gamma_1(t) = -\gamma_2(t) > 0$]. The decoherence rates and operators appearing in the electronic non-Markovian master equation are functions of the electronic coherence $C(t)$, and therefore depend on the parameter P_g . We have shown that the decomposition of $d\mathcal{P}/dt$ (electronic system's purity) appears as the sum of two subflows, one negative, corresponding to the positive decoherence rate, and one positive, corresponding to the negative decoherence rate, being significantly related to the non-Markovian behavior. The QFI flow dF_{P_g}/dt is a sum of three subflows, two of them being associated to the positive and negative decoherence rates. The time behavior of the QFI flow dF_{P_g}/dt , and its decomposition into subflows, were observed in a numerical simulation of the vibrational dynamics, relying on a specific molecular preparation in Cs_2 . We have examined the QFI flow dF_{P_g}/dt in relation to the non-Markovian behavior measured by the canonical measure $f(t) = |\gamma_2(t)|$, showing that dF_{P_g}/dt becomes positive when $f(t)$ increases. The connection between dF_{P_g}/dt and $f(t)$ is rooted in the time behavior of the electronic coherence, which is a reference quantity in defining the correlations between the electronic open system and its vibrational environment. All the three QFI subflows oscillate becoming positive and negative during the dynamics, showing different sources able to increase or decrease the information on the parameter P_g quantified by F_{P_g} . In the example illustrated by numerical results, the time behaviors of all QFI subflows are correlated to the non-Markovianity measure $f(t)$, but they can be easily differentiated, showing that they originate in distinct physical mechanisms. For example, the subflow $T_1(t)$ associated to $\gamma_1(t) > 0$ becomes positive for large values of $\gamma_1(t)$ and negative when $\gamma_1(t)$ has low values; the non-Markovian subflow $T_2(t)$ associated to $\gamma_2(t) < 0$ shows a very oscillating behavior when $f(t)$ reaches large values, and becomes negative when non-Markovianity is diminished; the subflow $T_3(t)$ is the dominant one in the QFI flow, $dF_{P_g}/dt \approx T_3$.

These results allow some general observations. In the framework proposed in this work, the information about the parameter θ is encoded in the open system, environment, and their interaction or/and correlations, being carried by the open

system dynamics. The dynamics of the QFI F_θ and its subflows reflect this sharing of information about θ , between an open system and an environment, which have θ as a common reference parameter. Therefore, specific mechanisms may increase or decrease the QFI flow and subflows in Markovian and non-Markovian dynamics. In the two specific examples treated here, the Markovian dynamics of a quantum probe, and the non-Markovian dynamics of an open system entangled with its environment, we have disclosed these mechanisms by relating the informational contents of the QFI flow and subflows to basic dynamic quantities and processes underlying the open system dynamics.

Let us highlight the reasons indicating that, in this case, the canonical measures of non-Markovianity provide a pertinent framework in addressing the connection between the QFI flow dF_θ/dt and non-Markovianity. One reason is that the canonical measure $f(\theta, t)$, defined from the negative decoherence rates, depends on the parameter θ and, therefore, the QFI flow dF_θ/dt is structurally related to the non-Markovianity measure $f(\theta, t)$. On the other hand, this framework allows to interrogate further the decomposition of the QFI flow into subflows associated with the decoherence rates. In Ref. [31] this decomposition disclosed a remarkable connection of the QFI subflows with non-Markovianity, as the positive QFI subflows were exclusively associated to the negative decoherence rates, and then to the information backflow from the environment to the open system. Here we have shown that the flow dF_θ/dt is composed of three types of subflows: subflows associated with positive and negative decoherence rates, and a third type coming through $\partial\rho/\partial\theta$. The part of the QFI flow related to non-Markovianity is the “non-Markovian QFI subflow” associated to the negative decoherence rates $\gamma_i < 0$. All these types of QFI subflows can become positive or negative during

the time evolution of the open system, increasing or diminishing the information about θ present in the system at a certain instant. One may consider a quantifier of “the information about θ entering in the system,” defined from the positive parts of the QFI flow dF_θ/dt :

$$\int_{dF_\theta/dt' > 0} \frac{dF_\theta}{dt'} dt'. \quad (103)$$

We have shown that all the QFI subflows may contribute to this quantifier; inside this total quantifier one can distinguish the non-Markovian contribution, coming from the positive parts of the non-Markovian QFI subflow.

Aside from their signs, the QFI subflows are enlightening because they differentiate the various sources of the information flow about the parameter. The non-Markovian example given here shows that, even if all the subflows can become positive and negative, they keep distinct temporal behaviors, reflecting their different physical origins.

We hope that this work will contribute in understanding the informational dynamics in cases where the dynamical relation between the open system and environment is mediated by a common parameter. This insight may be useful in cases when the open systems are used as quantum probes [63], or in metrological schemes “beyond the Cramér-Rao theorem,” where there is a dependence of the measurement strategy on the parameter [43].

ACKNOWLEDGMENTS

This work was supported by the Romanian Ministry of Research, Innovation and Digitization, through the Grant No. 16N/2019 within the National Nucleus Program, the LAPLAS VI Project No. PN 19150201.

-
- [1] C. W. Helstrom, *Quantum Detection and Estimation Theory* (Academic, New York, 1976).
 - [2] A. S. Holevo, *Probabilistic and Statistical Aspects of Quantum Theory* (North-Holland, Amsterdam, 1982).
 - [3] S. L. Braunstein and C. M. Caves, *Phys. Rev. Lett.* **72**, 3439 (1994).
 - [4] M. G. A. Paris, *Int. J. Quantum Inf.* **07**, 125 (2009).
 - [5] Y. Yang, G. Chiribella, and M. Hayashi, *Commun. Math. Phys.* **368**, 223 (2019).
 - [6] R. Demkowicz-Dobrzański, W. Górecki, and M. Guţă, *J. Phys. A: Math. Theor.* **53**, 363001 (2020).
 - [7] W. K. Wootters, *Phys. Rev. D* **23**, 357 (1981).
 - [8] I. Bengtsson and K. Życzkowski, *Geometry of Quantum States. An Introduction to Quantum Entanglement* (Cambridge University Press, New York, 2006).
 - [9] J. S. Sidhu and P. Kok, *AVS Quantum Sci.* **2**, 014701 (2020).
 - [10] G. Tóth and I. Apellaniz, *J. Phys. A: Math. Theor.* **47**, 424006 (2014).
 - [11] L. Pezzé, A. Smerzi, M. K. Oberthaler, R. Schmied, and P. Treutlein, *Rev. Mod. Phys.* **90**, 035005 (2018).
 - [12] D. Braun, G. Adesso, F. Benatti, R. Floreanini, U. Marzolino, M. W. Mitchell, and S. Pirandola, *Rev. Mod. Phys.* **90**, 035006 (2018).
 - [13] J. F. Haase, A. Smirne, J. Kołodyński, R. Demkowicz-Dobrzański, and S. F. Huelga, *Quantum Meas. Quantum Metrol.* **5**, 13 (2018).
 - [14] C. W. Helstrom, *Phys. Lett. A* **25**, 101 (1967); *IEEE Trans. Inf. Theory* **14**, 234 (1968).
 - [15] H. P. Breuer, *J. Phys. B: At. Mol. Opt. Phys.* **45**, 154001 (2012).
 - [16] A. Rivas, A. F. Huelga, and M. B. Plenio, *Rep. Prog. Phys.* **77**, 094001 (2014).
 - [17] H. P. Breuer, E. M. Laine, J. Piilo, and B. Vacchini, *Rev. Mod. Phys.* **88**, 021002 (2016).
 - [18] I. de Vega and D. Alonso, *Rev. Mod. Phys.* **89**, 015001 (2017).
 - [19] A. Smirne, J. Kołodyński, S. F. Huelga, and R. Demkowicz-Dobrzański, *Phys. Rev. Lett.* **116**, 120801 (2016).
 - [20] Y. Matsuzaki, S. C. Benjamin, and J. Fitzsimons, *Phys. Rev. A* **84**, 012103 (2011).
 - [21] A. W. Chin, S. F. Huelga, and M. B. Plenio, *Phys. Rev. Lett.* **109**, 233601 (2012).
 - [22] K. Bai, Z. Peng, H.-G. Luo, and J.-H. An, *Phys. Rev. Lett.* **123**, 040402 (2019).
 - [23] Y. Yang, *Phys. Rev. Lett.* **123**, 110501 (2019); A. Altherr and Y. Yang, *ibid.* **127**, 060501 (2021).
 - [24] W. Zhong, Z. Sun, J. Ma, X. Wang, and F. Nori, *Phys. Rev. A* **87**, 022337 (2013).

- [25] X. Hao, N.-H. Tong, and S. Zhu, *J. Phys. A: Math. Theor.* **46**, 355302 (2013).
- [26] K. Berrada, *Phys. Rev. A* **88**, 035806 (2013).
- [27] M. Ban, *Quantum Inf. Proc.* **14**, 4163 (2015).
- [28] Y.-L. Li, X. Xiao, and Y. Yao, *Phys. Rev. A* **91**, 052105 (2015).
- [29] H. R. Jahromi, *J. Mod. Opt.* **64**, 1377 (2017).
- [30] W. Wu and C. Shi, *Phys. Rev. A* **102**, 032607 (2020).
- [31] X.-M. Lu, X. Wang, and C. P. Sun, *Phys. Rev. A* **82**, 042103 (2010).
- [32] H. Song, S. Luo, and Y. Hong, *Phys. Rev. A* **91**, 042110 (2015).
- [33] J. Naikoo, S. Dutta, and S. Banerjee, *Phys. Rev. A* **99**, 042128 (2019).
- [34] Y.-N. Lu, Y.-R. Zhang, G.-Q. Liu, F. Nori, H. Fan, and X.-Y. Pan, *Phys. Rev. Lett.* **124**, 210502 (2020).
- [35] N. Mirkin, M. Larocca, and D. Wisniacki, *Phys. Rev. A* **102**, 022618 (2020).
- [36] M. Vatasescu, [arXiv:2012.10767v1](https://arxiv.org/abs/2012.10767v1).
- [37] M. J. W. Hall, J. D. Cresser, L. Li, and E. Andersson, *Phys. Rev. A* **89**, 042120 (2014).
- [38] D. A. Lidar, A. Shabani, and R. Alicki, *Chem. Phys.* **322**, 82 (2006).
- [39] J. Liu, X.-M. Lu, and X. Wang, *Phys. Rev. A* **87**, 042103 (2013).
- [40] H. Carmichael, *An Open Systems Approach to Quantum Optics* (Springer, Berlin, 1993).
- [41] M. A. Nielsen and I. L. Chuang, *Quantum Computation and Quantum Information* (Cambridge University Press, Cambridge, England, 2010).
- [42] M. Vatasescu, *Phys. Rev. A* **98**, 053426 (2018).
- [43] L. Seveso, M. A. C. Rossi, and M. G. A. Paris, *Phys. Rev. A* **95**, 012111 (2017).
- [44] F. Chapeau-Blondeau, *Phys. Rev. A* **91**, 052310 (2015).
- [45] S. Lorenzo, F. Plastina, and M. Paternostro, *Phys. Rev. A* **88**, 020102(R) (2013).
- [46] S. Jevtic, D. Newman, T. Rudolph, and T. M. Stace, *Phys. Rev. A* **91**, 012331 (2015).
- [47] L. Mancino, M. Sbroscia, I. Gianani, E. Roccia, and M. Barbieri, *Phys. Rev. Lett.* **118**, 130502 (2017).
- [48] A. Fujiwara, *Phys. Rev. A* **70**, 012317 (2004).
- [49] A. Fujiwara, *Phys. Rev. A* **63**, 042304 (2001).
- [50] A. Acín, E. Jané, and G. Vidal, *Phys. Rev. A* **64**, 050302(R) (2001).
- [51] H. Lefebvre-Brion and R. Field, *The Spectra and Dynamics of Diatomic Molecules* (Elsevier, Amsterdam, 2004).
- [52] M. Vatasescu, *Phys. Rev. A* **88**, 063415 (2013).
- [53] M. Vatasescu, *Phys. Rev. A* **92**, 042323 (2015); **93**, 069906(E) (2016).
- [54] M. Vatasescu, *J. Phys. B: At. Mol. Opt. Phys.* **42**, 165303 (2009).
- [55] E. Luc-Koenig, M. Vatasescu, and F. Masnou-Seeuws, *Eur. Phys. J. D* **31**, 239 (2004).
- [56] J. Cao, C. J. Bardeen, and K. R. Wilson, *Phys. Rev. Lett.* **80**, 1406 (1998); *J. Chem. Phys.* **113**, 1898 (2000).
- [57] M. Vatasescu, *Nucl. Instrum. Methods Phys. Res., Sect. B* **279**, 8 (2012).
- [58] M. Vatasescu, O. Dulieu, R. Kosloff, and F. Masnou-Seeuws, *Phys. Rev. A* **63**, 033407 (2001).
- [59] R. Kosloff, *Annu. Rev. Phys. Chem.* **45**, 145 (1994).
- [60] R. Kosloff, Quantum molecular dynamics on grids, in *Dynamics of Molecules and Chemical Reactions*, edited by R. E. Wyatt and J. Z. Zhang (Marcel-Dekker, New York, 1996), pp. 185–230.
- [61] K. Willner, O. Dulieu, and F. Masnou-Seeuws, *J. Chem. Phys.* **120**, 548 (2004).
- [62] L. A. Correa, M. Mehboudi, G. Adesso, and A. Sanpera, *Phys. Rev. Lett.* **114**, 220405 (2015).
- [63] P. Haikka and S. Maniscalco, *Open Syst. Inf. Dyn.* **21**, 1440005 (2014).
- [64] S. Bhattacharya, A. Misra, C. Mukhopadhyay, and A. K. Pati, *Phys. Rev. A* **95**, 012122 (2017).
- [65] S. Utagi, *Phys. Lett. A* **386**, 126983 (2021).